NSK Technical Journal

Motion & Control

No.15 December 2003

Hub Unit Bearings with ABS Sensor

ISSN1342-3630

NSK

MOTION & CONTROL No.15
NSK Technical Journal
Printed and Published: December 2003
ISSN1342-3630
Publisher: NSK Ltd., Ohsaki, Shinagawa, Tokyo, JAPAN
Public Relations Department
TEL +81-3-3779-7051
FAX +81-3-3779-7431
Editor: Hisashi MACHIDA
Managing Editor: Seizo SAITO
Design, Typesetting & Printing: Fuji Ad. Systems Corp.

Cover photos: Hub Unit Bearings with ABS Sensor

NSK Technical Journal
Motion & Control
No.15
December 2003

NSK

Contents

Hub Unit Bearings with ABS Sensor

Yuji Nakamura
Bearing Technology Center

ABSTRACT

NSK has developed wheel hub unit bearings that incorporate either a built-in wheel speed sensor or a separate wheel speed sensor rotor. These bearings can be categorized into four designs:

- Bearings with an annular passive sensor
- Bearings with a sensor between each row
- Bearings with a multi-pole magnetic encoder seal
- Bearings with an end-cap sensor.

In this article, we will discuss which sensor-integrated bearing design best serves a given application.

1. Introduction

As auto safety plays a more important role in vehicle design, manufacturers are expanding their efforts from passive safety to greater emphasis on active safety. Passive safety works to minimize damage to passengers when an accident occurs, while active safety works to prevent accidents from occurring in the first place.

Examples of active safety include anti-lock brake systems (ABS), which help prevent the wheels from locking during full braking, and traction control systems, which control wheel slippage during acceleration.

Automobile manufacturers are increasing such active safety systems in a greater number of their vehicles every year. For these systems to work effectively, the control unit of a traction control system or an ABS requires precise wheel speed measurements from each wheel.

As these systems become increasingly sophisticated, hub units must be able to provide wheel speed measurements with greater accuracy at low speeds.

To meet this growing demand, NSK has developed hub unit bearings that provide greater accuracy in wheel speed measurements.

2. ABS Technology Trends

The structures of conventional hub units are illustrated in Fig. 1 and 2. For driven wheels, the wheel speed sensor is secured to the knuckle, and the sensor rotor is press-fitted onto the outer ring of the constant velocity (CV) joint. For non-driven wheels, the wheel speed sensor is also secured to the knuckle, however, the sensor rotor is press-fitted onto the outer ring of the bearing.

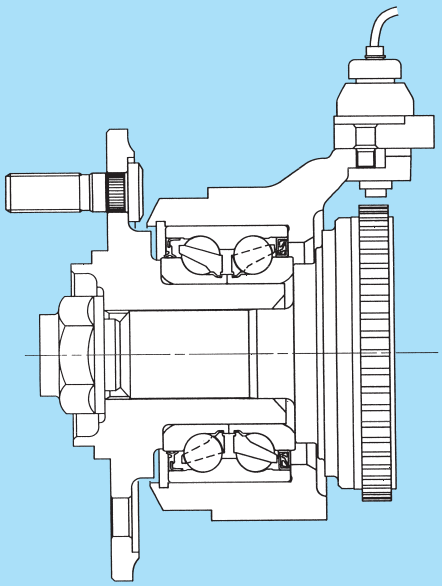

Fig.1 Conventional hub unit for driven wheel

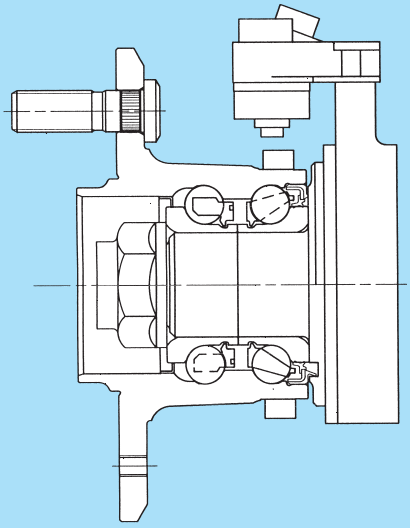

Fig. 2 Conventional hub unit for non-driven wheel

Table 1. Comparison of active and passive sensors

	Items	Passive sensor	Active sensor
Performance	Zero speed detection	Not possible	Possible
	Air gap size	Restricted (due to size of sensor)	Large
Mechanical element	Compact/Lightweight	Difficult (due to large magnet)	Possible (due to small MR device)
	Unitization of seal and sensor rotor	Difficult (output signal of small sensor rotor is too small)	Possible
	Simplified sensor assembly	Possible (Only for integrated type bearings)	Possible (Clip-on type sensor carrier is used.)
	Standardization of sensor design	Difficult (due to unique element device design)	Possible
ECU	Waveform shaper	Required	Not required

The wheel speed sensor is a passive sensor that consists of a permanent magnet, a pole piece, and a coil. Induced voltage from the magnetic sensor generates an output signal that increases in both frequency and amplitude with wheel speed. The amount of voltage produced is also directly related to the distance between the sensor and the sensor rotor. This distance is known as the “air gap”.

Recently, however, hub units using an active sensor are increasing. Unlike a passive sensor, active sensors take advantage of semiconductor technology. Table 1 provides a comparison of both passive and active sensors.

3. Hub Unit Bearings with an ABS Sensor

For a conventional layout, the passive sensor type poses the following challenges:

A. Low wheel speed: Since amplitude and frequency of the output signal are in direct proportion to wheel speed, as the output signal decreases at low speed, it becomes difficult to measure the wheel speed.
B. Large sensor: Dimensions of the magnet, pole piece, and coil are relatively large.
C. Guaranteeing output signal from the sensor: Output signal of the sensor cannot be checked until the vehicle has been fully assembled, thus making it difficult to make repairs if a faulty component is found.

To address these challenges, we have developed bearings with a built-in sensor rotor and bearings with a built-in sensor rotor and sensor.

As for the type of sensor, we have made several developments that include use of either a passive sensor or an active sensor. Our newly developed bearings can be classified as follows:

- Bearings with an annular sensor
- Bearings with a sensor between each row
- Bearings with a multi-pole magnetic encoder seal
- Bearings with an end-cap sensor

The features of each type are further explained here.

3.1 Bearings with an annular sensor

This bearing (Fig. 3) is compact, lightweight, and designed to provide efficient use of available space. The output signal of the sensor is strong enough for detecting low wheel speeds with a passive sensor.

The toothed sensor ring consists of a magnet, a coil, and two pole pieces. The number of teeth of the sensor ring equals the number of pulses required for one rotation. The entire surface of the sensor ring is read by the sensor, and faces the sensor rotor. The sensor rotor is made of a press-molded steel plate, which has equally spaced rectangular windows that are open at the sensor-reading sections.

Since the sensor reads the entire outside surface, the air gap is averaged in the event the sensor rotor becomes deformed, or if there is excessive suspension jounce and rebound. This ensures a stable amplitude and frequency of the output signal.

The sensor is fixed to a cap, which is press-fitted onto the outer ring. This structure makes it quite suitable for the non-driven wheel.

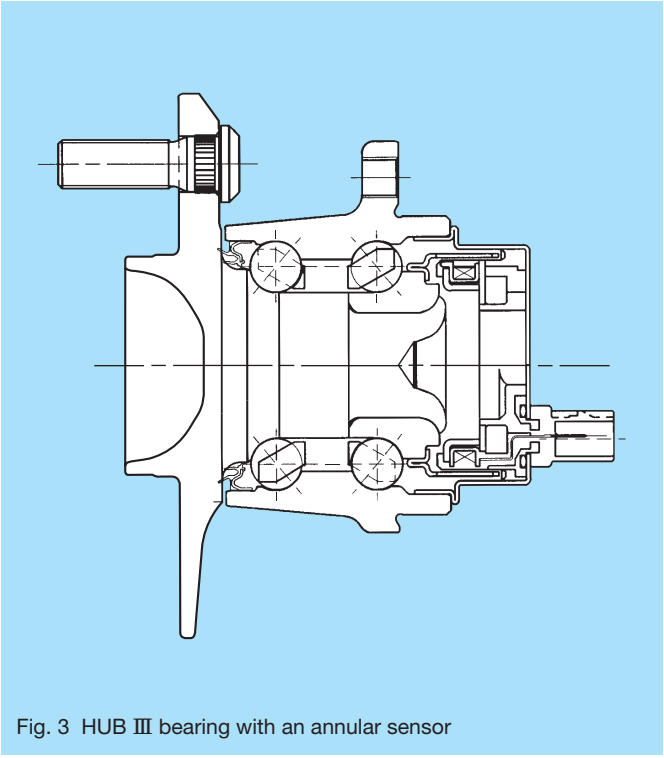

Fig. 3 HUB Ⅲ bearing with an annular sensor

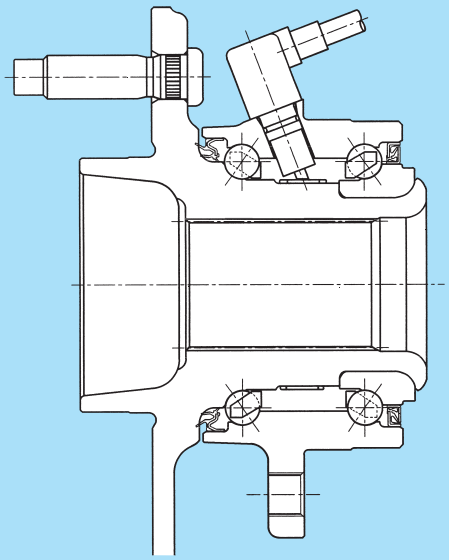

Fig. 4 HUB Ⅲ bearing with the sensor between each row

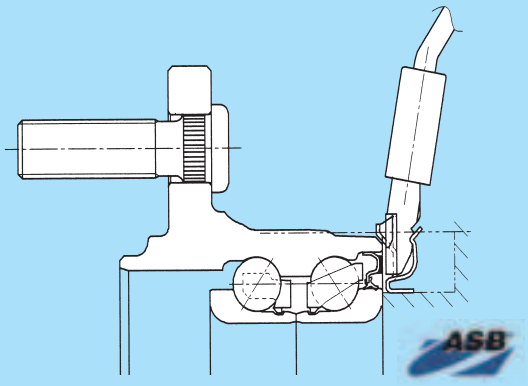

Fig. 5 HUB Ⅱ bearing with the multi-pole magnetic encoder seal

3.2 Bearings with a sensor between each row

This bearing (Fig.4) comes with a built-in sensor that is located between the two rows of rolling elements. The built-in sensor can be either passive or active. After making a hole in the outer ring, the sensor, which is cylindrical, is inserted through the hole and secured by a bolt. The sensor rotor is press-fitted onto the inner ring. Since the sensor is located between the two rows, there is minimal fluctuation of the air gap during excessive suspension jounce and rebound. Furthermore, since the dispersion of the air gap at the assembly stage can be controlled to a minimum, even a small passive sensor can be used. This sensor can be used with either the driven wheels or the non-driven wheels, but is especially beneficial to driven wheels where there are space limitations.

3.3 Bearings with a multi-pole magnetic encoder seal

This bearing (Fig. 5) comes with a built-in multi-pole magnetic encoder seal. Conventional passive sensors and geared sensor rotors can be easily replaced with a built-in multi-pole magnetic encoder seal, since the sensor and the sensor rotor can be made very compact without requiring any drastic design change to the surrounding area of the bearing. If the size of the sensor rotor and the number of pulses per rotation are designed appropriately, a permissible air gap can be made larger thus improving reliability. Our multi-pole magnetic encoder seal consists of multi-pole magnetic rubber that is vulcanized to a metal ring. There are two types of multi-pole magnetic encoder seals: an axial type, which is a disc-shaped rubber magnet, and radial type, which is a ring-shaped rubber magnet. They are classified into two types: a sensor-rotor-seal type is unitized with a seal, and a stand-alone type, which has

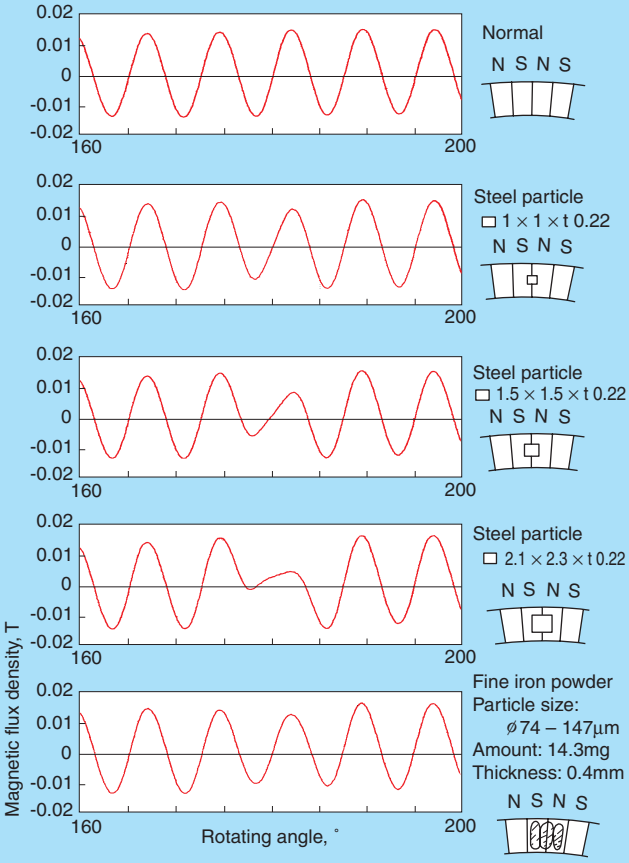

Fig. 6 Influence of magnetic particles

a separate sensor-rotor. Both types are press-fitted onto the outside diameter of the rotating ring.

Since sensor rotors are exposed to the external environment, the hub unit design needs to be able to protect the sensor rotors from various elements, especially magnetic particles. Small magnetic particles have little influence on sensor rotor function. However, if the particles are very large, or their amount becomes too excessive, they can impact magnetic flux density, and affect the amplitude and frequency of the output signal. Fig. 6 shows how intrusion of magnetic particles can influence encoder performance. In order to prevent the ingress of magnetic particles, we designed a labyrinth structure around the sensor rotor, which ensures that our multi-pole magnetic encoder seal is suitable for either driven wheels or non-driven wheels.

3.4 Bearings with an end-cap sensor.

Fig. 7 shows an end-cap sensor that is attached to a hub unit bearing for a non-driven wheel. End cap sensors can be easily designed for bearings with a built-in annular sensor for integration with non-driven wheel bearings. Two types of sensor are available: separated and unitized. The separated type consists of cylindrical-shaped sensor attached to a cap, and the unitized type is integrated with a cap. The separated type can be mass-produced for enhanced cost performance and easy replacement of the sensor. The unitized type is compact, lightweight, and highly reliable. Both types of sensor rotor are designed with features that protect them from the surrounding environment, including magnetic particles. Furthermore, a small air gap between the sensor and the sensor rotor is maintained for improved output signal accuracy. Bearings with the end-cap type sensor can be either active type or passive type.

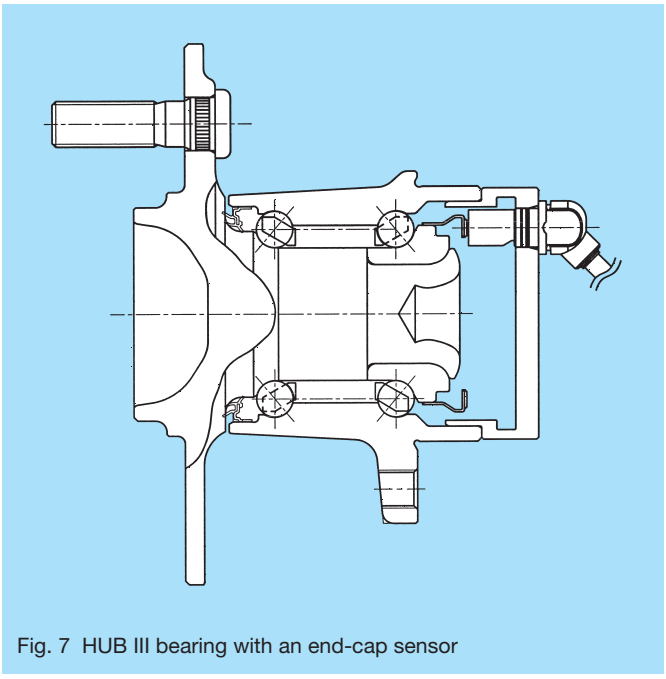

Fig. 7 HUB III bearing with an end-cap sensor

4. Conclusion

The need for bearings with built-in sensors is expanding to include greater adoption of active sensors.

NSK provides customers with optimum specifications for each application for all four types of bearings with built-in sensors.

Yuji Nakamura

Development of NSK ABLE Forecaster

Seigou Urakami, Corporate Research and Development Center
Hiromichi Takemura, Bearing Technology Center

ABSTRACT

Today, the operating conditions of bearings are diverse and therefore it is difficult to calculate the life of a bearing using the conventional rolling element bearing equation. To solve this problem, NSK has developed an original new life equation called "NSK ABLE Forecaster" and is as follows:

$L_{able}=a_1 a_{NSK} L_{10}$

The new life modification factor a_{NSK} takes into consideration the effects of lubrication conditions, the degree of lubricant cleanliness, fatigue limit, and material properties including heat treatment. In addition, the new life equation is based on actual data obtained from tests carried out on over 450 roller bearings and over 550 ball bearings under a variety of operating conditions.

As a result the NSK ABLE Forecaster provides a more accurate predication of bearing life.

Now NSK ABLE Forecaster is available on the NSK Web Page, http://www.nsk.com/index2.html.

1. Introduction

Bearings operate in a variety of situations in the field, ranging from contaminated lubricant conditions to high vacuum and clean environments. This has posed a significant challenge in trying to accurately predict bearing life using a conventional bearing life equation. To address this issue, NSK developed a new life equation program called the NSK ABLE Forecaster.

NSK ABLE Forecaster (Version 1.0), which was released on CD-ROM in August 2000, more accurately calculated rolling bearing life based on actual operating conditions. NSK released Version 2.0 in 2002, and has made it available to customers at the NSK website (www2.jp.nsk.com/BearingGuide/). Concept, contents, and operating method of NSK ABLE Forecaster are introduced in this article.

2. New Life Equation Program —NSK ABLE Forecaster

Conventional bearing life calculations are based on the Lundberg and Palmgren theory. This theory calculates life as it relates to subsurface-originated flaking, which assumes that cracks generated by the dynamic shearing stress under a rolling contact surface develop to the surface and lead to flaking. NSK ABLE Forecaster goes further and includes both subsurface-originated flaking and surface-originated flaking.

For subsurface-originated flaking, we developed Equation (1) by considering both the fatigue limit shown in Fig. 1 and the conventional Lundberg and Palmgren theory.

$$\ln \frac{1}{S} \propto N^e \int_V \frac{(\tau - \tau_u)^c}{Z_0^h} dV \quad \cdots\cdots (1)$$

Equation (2) shows the bearing life calculation for surface-originated flaking.

$$\ln \frac{1}{S} \propto N^e \int_V \frac{(\tau - \tau_u)^c}{Z_0^h} dV \times \left(\frac{1}{f(a_c, a_L)} - 1 \right) \quad \cdots\cdots (2)$$

Equation (3) is the sum of Equation (1) and Equation (2).

$$\ln \frac{1}{S} \propto N^e \int_V \frac{(\tau - \tau_u)^c}{Z_0^h} dV \times \left(\frac{1}{f(a_c, a_L)} \right) \quad \cdots\cdots (3)$$

From Equation (3), we can obtain Equations (4) and (5).

$$L_{able} = a_1 a_{NSK} L_{10} \quad \cdots\cdots (4)$$

$$a_{NSK} \propto f\left[\frac{P - P_u}{C} \cdot \frac{1}{a_c}, a_L \right] \quad \cdots\cdots (5)$$

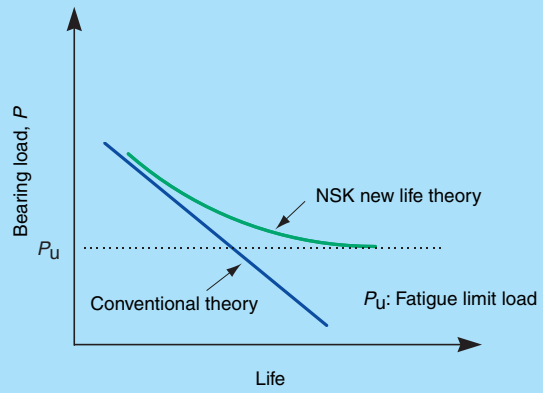

Fig. 1 NSK new life theory utilizing fatigue load limit

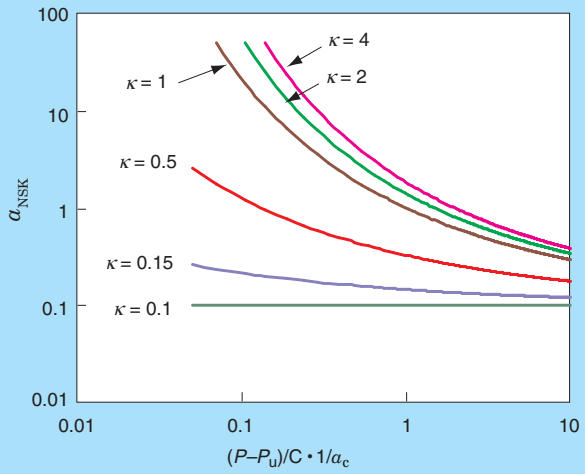

Fig. 2 Life modification factor "a_{NSK}" curves for ball bearings

Where:
S: Ratio not generating flaking at N cycles of stress load
N: Number of stress cycles
τ: Internal stress
τ_u: Internal stress of fatigue limit load
V: Stress volume
Z_0: Depth of maximum shearing stress
a_c: Contamination factor
a_L: Lubrication factor (function of viscosity ratio κ)
P: Bearing load
P_u: Fatigue load limit
C: Basic dynamic rating load
e, c, h: Constants

Fig. 2 illustrates Equation (5).

2.1 Subsurface-originated flaking

Generation of subsurface-originated flaking of rolling bearings assumes that a sufficient oil film always exists between rolling elements and the raceway surface under clean lubricating conditions. Fig. 3 shows the plotted L_{10} life for eight test conditions. Maximum contact surface pressure (P_{max}) is shown in the vertical axis, repeated stress cycles are shown in the horizontal axis, and the straight line represents L_{10} theoretical life. In actual testing, maximum contact surface pressure decreased, and actual bearing life departed from the calculated data of the conventional life theory towards a longer life. This figure shows that there is a fatigue limit under which rolling fatigue does not occur.

2.2 Surface-originated flaking

There are many cases where lubricant is contaminated by the ingress of foreign particles in rolling bearings under actual operating conditions.

When lubricant is contaminated with foreign particles, the foreign particles become compressed between the raceway surface and rolling element contact area, causing formation of a dent on both the raceway surface and rolling contact surface. Stress concentration occurs at the edge of the indentation resulting in minute cracks that initiate flaking. When maximum contact surface pressure is reduced, actual bearing life departs from the calculated data of the conventional life theory towards a shorter life as shown in Fig. 4. This shows that actual bearing life under contaminated lubrication cannot be significantly lengthened even if the maximum contact surface pressure is reduced.

We classified the lubricating conditions into five categories and decided on a contamination factor (a_c) as shown in Table 1.

Whereas bearing life depends on how well an oil film is formed, NSK ABLE Forecaster includes variables for

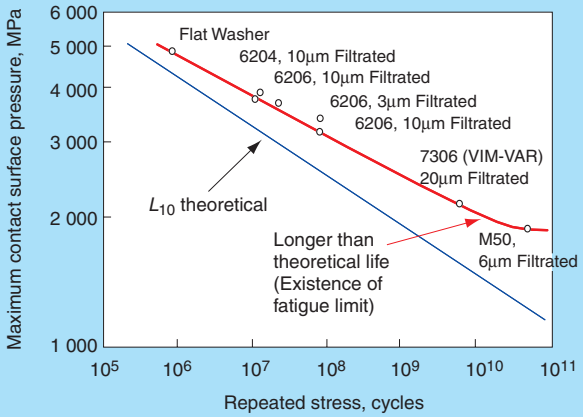

Fig. 3 Results of life test under clean lubrication

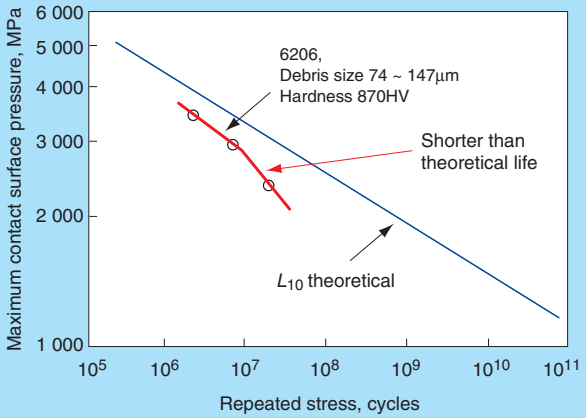

Fig. 4 Results of life test under contaminated lubrication

Table 1 Contamination factor

Cleanliness	Very clean	Clean	Normal	Contaminated	Heavily contaminated
α_c factor	1	0.8	0.58	0.4 ~ 0.1	0.05
Application standard	–10 μm filtered	10 – 30 μm filtered	30 – 100 μm filtered	100 μm – filtered or not filtered (Oil bath, circulating lubrication, etc.)	• Not filtered • Presence of particulate contamination
Application examples	• Sealed grease-lubricated bearings for electrical appliances and information technology equipment	• Sealed grease-lubricated bearings for electric motors, railway axle boxes and machine tools	• Normal-use bearings • Automotive hub unit bearings	• Automotive transmissions • Reduction gears • Construction machinery	

operating temperatures, and viscosity ratio κ (operating viscosity ν / required viscosity ν_1) to determine life. Required viscosity means kinematic viscosity in which the life correction factor is 1 at L_{10} $(C/P)^p$ in the ASME database, which can be obtained from the pitch circle diameter d_m and speed n of the bearing. In addition, operating viscosity means kinematic viscosity at operating temperatures.

Fig. 5 shows examples of NSK's long life bearing technologies. Bearing material is closely related to long bearing life in addition to using the proper material for specific load conditions and operating environments. NSK ABLE Forecaster accurately reflects the relation between bearing material and bearing life.

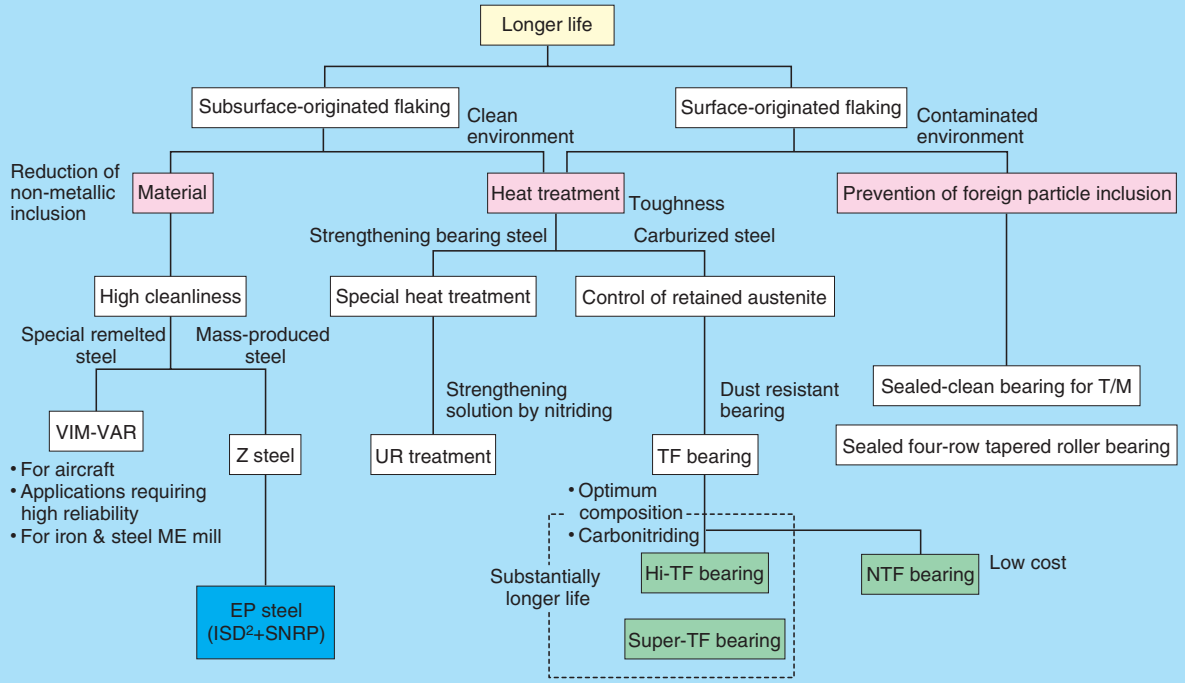

Fig. 5 Examples of NSK's long bearing life technology

3. NSK ABLE Forecaster on the Web

Version 1.0 of the new life equation program, NSK ABLE Forecaster, was released on CD-ROM in August 2000. Two years later, Version 2.0 was made accessible from the NSK website. Instructions on how to use the online version of NSK ABLE Forecaster are explained below.

The program consists of the following:

- Bearing life calculation
  Designate a bearing number
  Designate bearing numbers (Maximum 10 bearing numbers)

- Bearing selection according to required life

Fig. 6 NSK ABLE Forecaster—Calculations for a selected bearing

Fig. 7 NSK ABLE Forecaster—Calculation results

Fig. 6 shows the main window for designating a bearing number. A bearing number is selected from the bearing selection screen that links to the NSK Rolling Bearings Catalog database. Bearing life L_{able} and viscosity ratio κ can be obtained by following the procedure shown below (Fig. 7):

- Type the radial load, axial load, speed, and ratio of operation.
- Select reliability, load factor, and lubricant (grease or oil).
- Select a contamination factor. Type an operating temperature.
- Select a bearing material/special specification.
- Click **Calculate**:

Example of calculation

1. Open your web browser. (This example uses Microsoft® Internet Explorer.)
2. Go to the following address: www2.jp.nsk.com/BearingGuide/
3. Click **English**. Click **Bearing number** or **Bearing type**.
4. Type 6206 under Search by bearing number and click **Search**.
5. Click **List Details**, and then **Calculate**.
6. Click **Calculation for a Selected Bearing** under the Calculation menu.
7. Type 3120 for radial load, 0 for axial load, 3900 for speed, and 100 for ratio of operation in the text boxes.
8. Type 80 for operating temperature, and select ISO

Fig. 8 NSK ABLE Forecaster—Life calculations adjusted for specified variables

VG68 for Lubricant (Oil).

9. Select Normal (0.5) for Contamination factor a_c.
10. Select 100Cr6/100CrMnSi4-4 standard for Bearing material/Special specification, then click **Calculate**.

The following results are obtained:
κ=1.3
a_{NSK}=4.84
L_{able} =5052 hours (L_{10}=1043 hours)

By clicking **Calculate life for conditions**, you can change various operating conditions (load, speed, contamination factor, operating temperature, lubrication oil) for comparison with the originally specified conditions.

Click **Calculate** and a graphic illustration will show the results of changing lubrication oil ISO VG7 to ISO VG460 (283 hours to 12330 hours). This allows you to check a variety of parameters when the load or viscosity grade of lubrication oil is changed or when the degree of contamination is changed by use of a different filter.

4. Conclusion

NSK ABLE Forecaster expands on the conventional bearing life equation, by addressing both subsurface-originated flaking and surface-originated flaking to theorize a new life calculation program. NSK has taken full advantage of years of empirical test data and analysis results of products actually used in the field to develop superior bearing life prediction. NSK ABLE Forecaster Ver. 2.0 is available in its entirety for our customers and prospective clients on the World Wide Web.

We will continue to make further enhancements to NSK's already highly functional new life calculation program, NSK ABLE Forecaster. We expect to continue our research and developments for even more accurate calculations and easier operations by users.

Seigou Urakami

Hiromichi Takemura

Long Life Bearing Technology by Carbonitriding

Yasuo Murakami
Corporate Research and Development Center

ABSTRACT

This report presents a technique for reducing fatigue caused by rolling contact under contaminated lubrication. We have developed a material that maintains high hardness despite containing a large amount of retained austenite. By combining new SAC steel and carbonitriding heat treatment technologies, we have produced a new bearing material. The key to our success lies in successfully dispersing of a large number of fine carbonitride particles. Applications born out of this study include both the Super TF Bearings and Hi-TF Bearings. These bearings continue to enjoy long life under severe lubrication conditions.

1. Introduction

Rolling bearings are indispensable machine elements that maintain smooth rotation and support a rotating shaft under severe operating conditions of heavy loads and high speeds. They operate in a variety of extremely severe environments, which may include lubricating oil that is contaminated with foreign matter such as fine iron powder and dirt from the casting of the casing.

In the market, rolling bearings are commonly used under contaminated lubrication conditions in differential gears or transmissions where long service life is of the utmost importance. Bearings used under contaminated lubrication conditions suffer from indentations or scratches that are generated on the raceways by foreign particles, which initiate cracks or flaking.

We conducted research on material that contains a large amount of retained austenite and maintains high hardness from the viewpoints of material and heat treatment (carbonitriding treatment), and developed Super TF bearings and Hi-TF bearings as a measure against bearing failure. Our results are reported here.

2. Surface-Originated Flaking

Surface-originated flaking is generated under conditions of lubricant mixed with fine iron powder or dirt from the casting of the casing, and is initiated at the edge of an indentation. The process that initiates the generation of surface-originated flaking (Fig. 1) begins with a crushing action of foreign particles, which generates indentations. Stress concentrations around the surface indentations create cracks around the indentation, which progress into cracks that lead to flaking.

Therefore, in order to extend service life of rolling bearings, we must reduce the stress concentrations around each surface indentation.

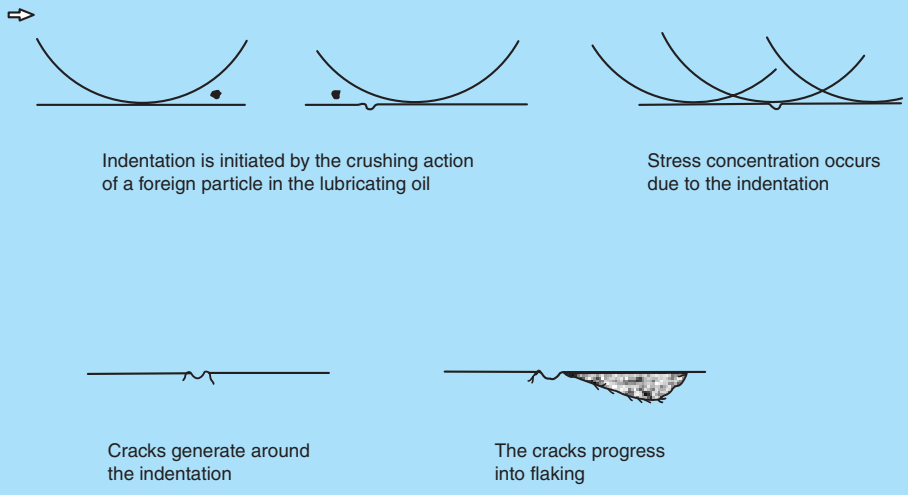

Fig. 1 Process of surface-originated flaking

3. Minimizing Stress Concentrations

Fig. 2 illustrates contact stress concentrations at the edges of an indentation that can be expressed by [$P/P_0 \propto (r/c)^{-0.24}$], which is a function of r/c, and suggests that the larger the r/c, the smaller the stress concentration and ultimately longer life[1]. Here, r is the curvature around a surface indentation, and c is the radius of indentation.

The r/c value indicates that a technique for controlling the shape of an indentation is important.

For the relationship between the r/c value and the material, we conducted research using Vickers indentations as dummy indentations[2)3)]. Based on our results, the strongest relationship shown with the r/c value is the amount of retained austenite. As the amount of retained austenite increases, the r/c value becomes larger, and the reduction of stress concentrations is enhanced.

In efforts to further enhance service life under contaminated lubrication conditions, it became clear that material with a higher concentration of retained austenite and high hardness is the best material for reducing stress concentrations around a surface indentation. However, retained austenite has a soft structure, which reduces the hardness of the bearing material. In order to meet the seemingly conflicting needs for greater hardness of the bearing material and a higher level of retained austenite, we developed a technique (TF technology) that promotes the formation and uniform distribution of appropriate quantities of carbonitride particles in the bearing material. NSK's TF technology combines SAC steel with carbonitriding heat treatment technology.

Photo 1 shows the surface structure of bearing material with uniform distribution of fine carbonitride particles obtained with the new TF technology. For comparison, Photo 2 shows the surface of conventional bearing steel with standard carburized structures. Fig. 4 shows the relation between hardness and the amount of retained austenite. As the amount of retained austenite increases in conventional bearing steel, hardness is lowered as indicated in the range between the dotted lines. In contrast, Super TF material with uniform distribution of finer carbonitride particles gives Super TF bearings greater hardness (HV 70 to 80) and higher retained austenite levels than TF bearings.

Fig. 5 shows the relationship between the r/c value and repeated stress. This figure reflects the results of a Vickers indentation test that was performed on a rolling surface using a steel ball to apply repeated stress. The r/c value was measured in chronological order. The carburized bearing showed an increased amount of retained austenite and a larger r/c value than that of the SAE 52100 bearing. The Super TF bearing with its greater hardness and uniform distribution of fine carbonitride particles achieved a higher r/c value than that of a carburized bearing with only increased retained austenite. Fig. 5 shows the result of repeated stress testing at 3 000 cpm. The r/c value remained constant after only 3 to 5 minutes.

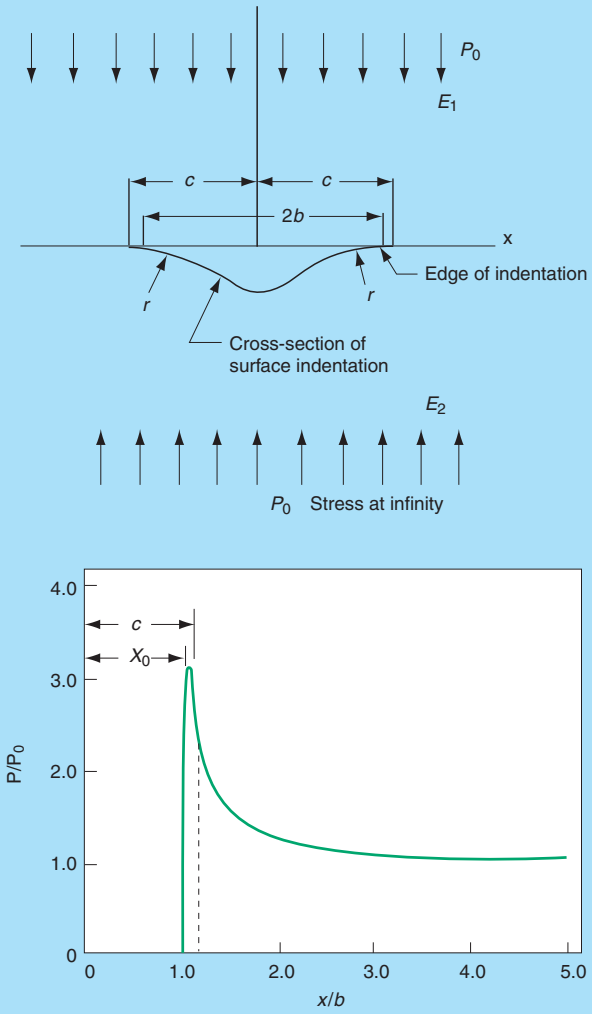

Fig. 2 Stress concentrations around surface indentations[1)]

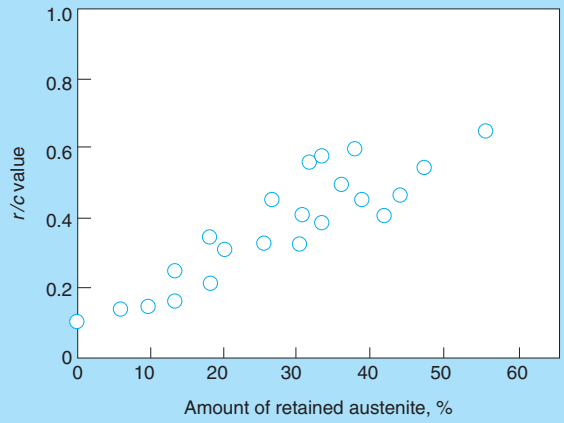

Fig. 3 Relationship between r/c value and amount of retained austenite

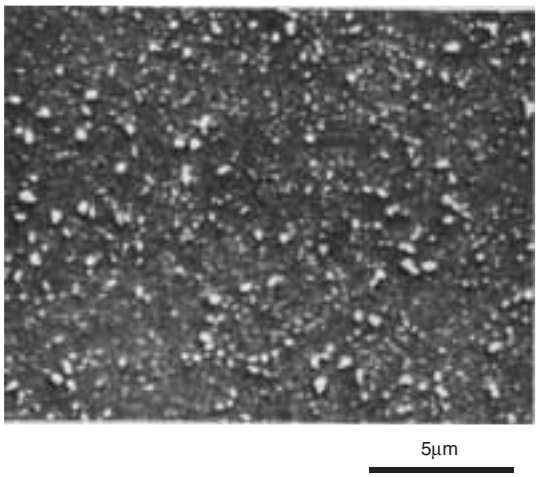

Photo 1. Microstructure of carbonitrided SAC steel

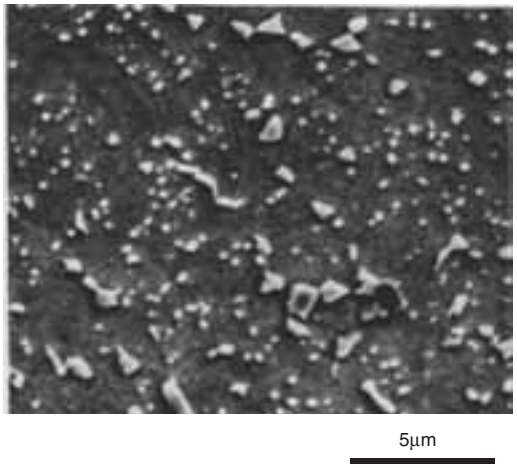

Photo 2. Microstructure of carburized conventional steel

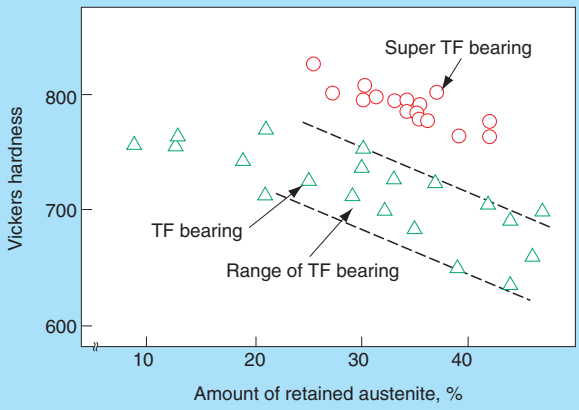

Fig. 4 Relationship between material hardness and retained austenite level

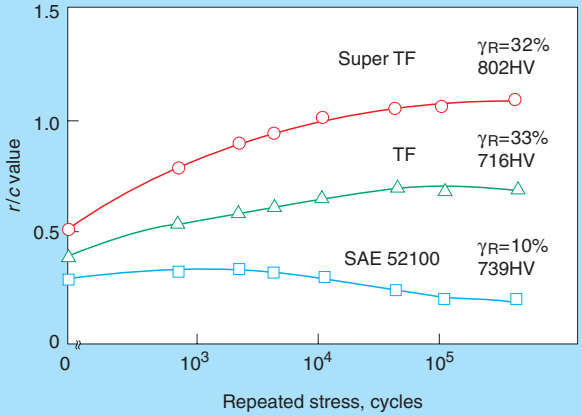

Fig. 5 Change of r/c value under repeated stress

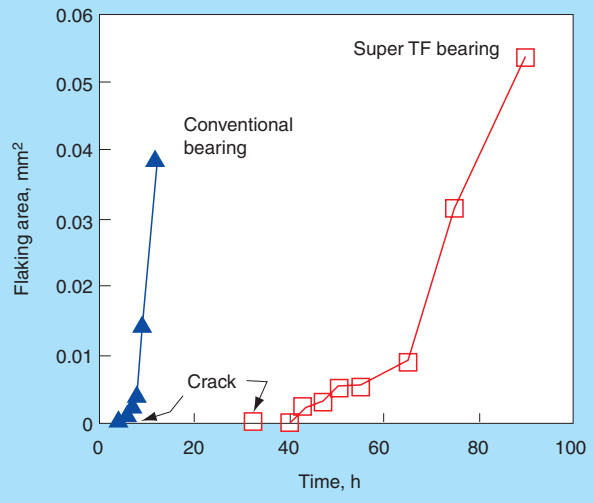

Fig. 6 Crack initiation and flaking area

Fig. 6 shows the progress of flaking. Compared to a conventional bearing, our Super TF bearing shows longer resistance to crack initiation near surface indentations with flaking progressing at a much slower pace.

4. Fatigue Life under Contaminated Lubrication

A flat washer type (FWT) life test using disks made of carburized TF bearing material and a Super TF bearing material under contaminated lubrication was conducted. Fig. 7 shows the structure of the FWT test rig with an improved design to ensure constant supply of contaminants to the trace.

Test conditions:
N = 3 000 cpm
P_{max} = 4 900 MPa

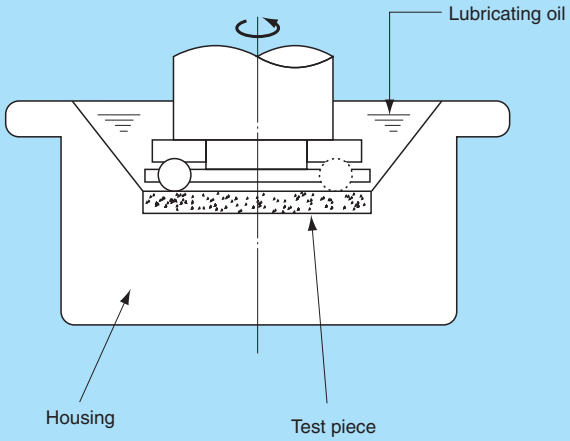

Fig. 7 Improved flat washer type RCF test rig

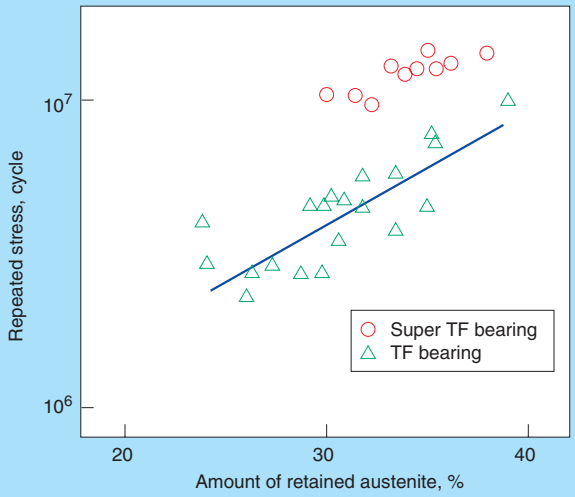

Fig. 8 Relationship between fatigue life (L_{10}) and amount of retained austenite under contaminated lubrication

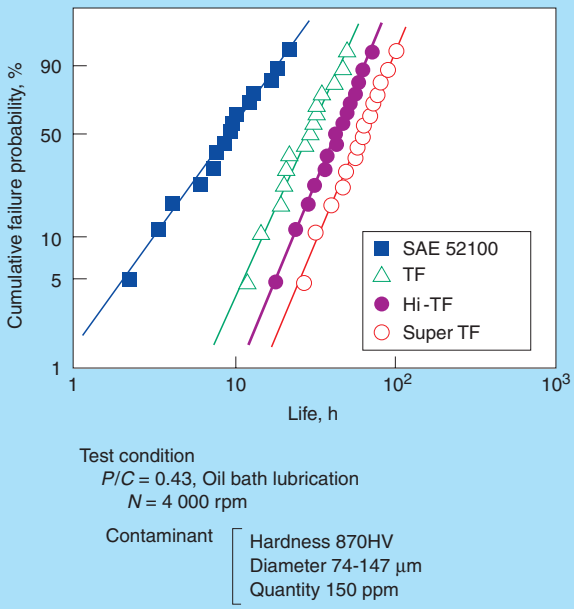

Fig. 9 Life test results of tapered roller bearings with contaminated lubrication

Lubrication = Turbine oil VG68
Contaminant hardness: 540HV
Diameter: 74 to 147 µm
Quantity: 300 ppm

Fig. 8 shows that fatigue life under contaminated lubrication depends on the amount of retained austenite. In this figure, ○ represents the L_{10} life of carburized bearings (Super TF bearings) as obtained from ten tested samples. △ represents the L_{10} life of TF bearings.

Bearings with increased retained austenite achieved longer service life under contaminated lubrication. Super TF bearings, for which the *r/c* value was higher by increasing hardness with the same amount of retained austenite as carburized bearings, showed longer life by more than 10^7 cycles.

Life test results for tapered roller bearings L44649/10 under contaminated lubrication are shown in Fig. 9. Compared to standard carburized bearings, the Hi-TF bearings and Super TF bearings achieved a service life that was more than five times longer.

5. Conclusion

In order to achieve longer bearing life under contaminated lubrication, it was necessary to develop a material that maintains high hardness despite containing large amounts of retained austenite. NSK succeeded in developing a breakthrough carbonitriding technology that promotes the formation and uniform distribution of appropriate quantities of carbonitride particles in the bearing material.

Super TF bearings and Hi-TF bearings developed with this new technology are used in various automotive applications. Their long service life is being proven in the marketplace. We anticipate further expansion of Super TF bearings and Hi-TF bearings for applications requiring long life while operating under contaminated lubrication.

References:

1) Y. P. Chiu, J. Y. Liu, "An Analytical Study of the Stress Concentration Around a Furrow shaped Surface Dent in Rolling Contact," Transaction of ASME, 92 (1970) 258.
2) Y. Murakami, Y. Matsumoto, K. Furumura, "Research of long life bearing material under contaminated lubrication," Japanese Society of Tribology (1988) 297-300
3) Y. Murakami, Y. Matsumoto, K. Furumura, "Long life TF bearing under Contaminated Lubrication," NSK Technical Journal, 650 (1989) 1-11
4) K. Furumura, Y. Murakami, T. Abe, "The Development of Bearing Steels for Long Life Rolling Bearings Under Clean Lubrication," ASTM-STP1195 (1993) 199-210
5) Y. Murakami, N. Mitamura, K. Furumura, "Long life Super-TF Bearing and Hi-TF Bearing under Severe Lubrication," NSK Technical Journal, 652 (1992) 9-16

Yasuo Murakami

Research of Auxiliary Landing Bearings for Turbo Molecular Pumps

Yukio Oura and Sumio Sugita
Corporate Research and Development Center

ABSTRACT

Recently, various industries require high-vacuum environments for highly technical precision applications. A turbo molecular pump is a high-vacuum device designed to achieve approximately 10^{-8}Pa, and consists of several components including high-speed magnetic bearings. In the event that electric power is cut off from the magnetic bearing for any unexpected reason, load capacity is immediately lost. The rotor and the stator abruptly make contact with each other resulting in complete failure of the pump. In order to protect the pump and magnetic bearings, auxiliary landing or "touchdown" bearings are incorporated into the pump design. NSK investigated shaft behavior of a pump, and by determining the amount of load applied to the bearings, we discovered some important aspects that would aid us in developing a more durable and thermal stress resistant auxiliary landing bearing.

1. Introduction

Turbo molecular pumps with magnetic bearings are widely adopted to meet high-vacuum requirements, which can attain vacuum levels of approximately 10^{-8} Pa.

In the event of sudden power loss to the magnetic bearings, load capacity is lost immediately. The rotor and the stator come into contact with each other resulting in complete failure of the pump. Therefore, rolling bearings functioning as auxiliary bearings are used to protect the pump and the magnetic bearings from damage.

Whereas auxiliary bearings operate in a vacuum environment, heat that has been generated is difficult to diffuse, resulting in bearings that are apt to have very localized hot spots. In addition, when auxiliary landing bearings supporting the rotor experience abrupt acceleration from the maximum rotating speed during high-speed delevitation, they are also exposed to severe load conditions during such an abrupt acceleration[1], which potentially leads to bearing damage or failure. Our task was to determine how to improve the durability of auxiliary bearings under such operating conditions. However, factors such as heat and load made it difficult to fulfill our task. We realized it was not enough for us to only understand the probable causes of bearing failure. We thus tried to estimate the amount of load applied to the bearing by focusing and analyzing shaft behavior of an actual pump.

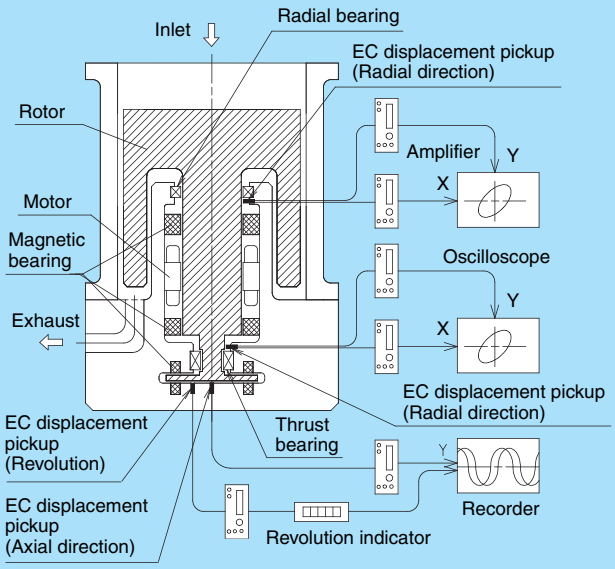

Fig. 1 Turbo molecular pump

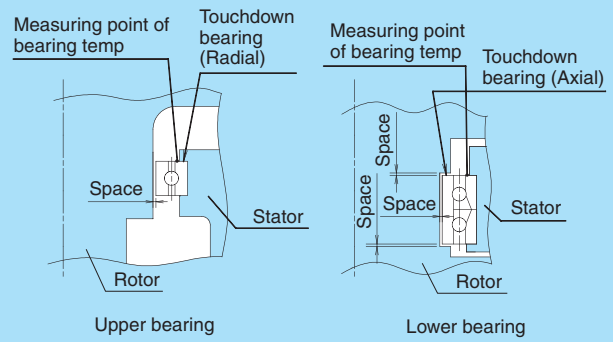

Fig. 2 Auxiliary landing bearings

2. Delevitation Test

2.1 Test method

Our first test (Table 1) consisted of an actual pump, which was vertically mounted. The pump rotor was allowed to delevitate or coast to a stop, down from the maximum speed. This was repeated until abnormal signs of endurance, rotating speed, and sound were detected. Measured items consisted of shaft rotating speed,

Table 1 Test conditions and test bearings

No.			Test bearings				
No.	Vacuum (Pa)	Rotating speed (rpm)	Position	Bore size (mm)	Type	Material	Coating
1	10^{-1}	21 600	Upper	ø110	Full complement ball bearing (No cage)	Rings: SUS440C Balls: Si_3N_4	MoS_2 (Inner ring and balls)
			Lower	ø60			
2		32 000	Upper	ø60	Full complement ball bearing (No cage)	Rings: SUS440C Balls: Si_3N_4	MoS_2 (Inner ring and balls)
			Lower	ø25			

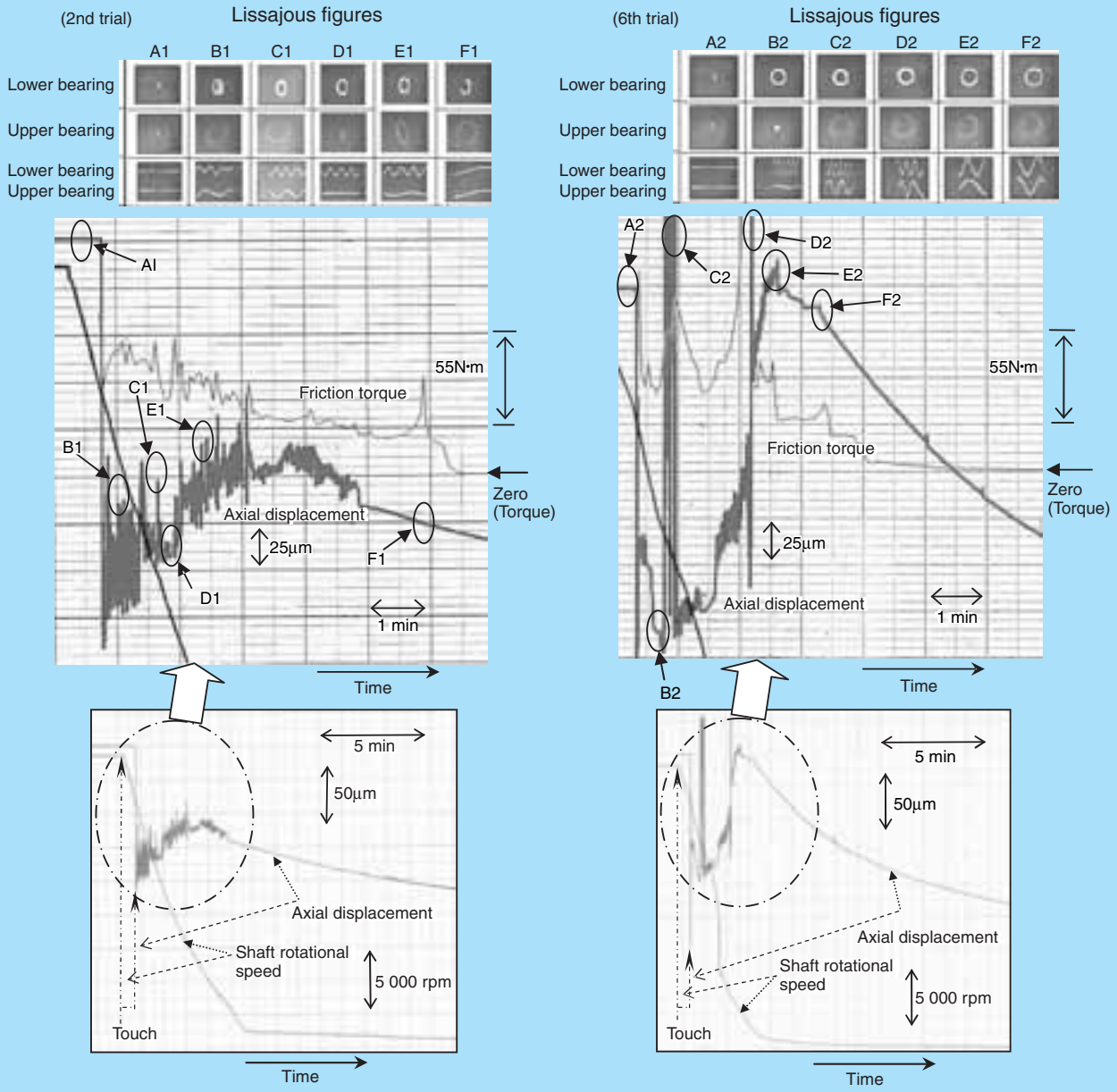

Fig. 3 Experimental and calculated results

displacement of both upper and lower bearings in the radial direction, and axial displacement of the shaft. Fig. 1 shows the locations of the sensors. Analysis of shaft behavior was completed only for the first test.

In the second test, (Table 1), the rotor of a different type of vertically mounted pump was delevitated at full speed, and the outer ring temperatures of the upper and lower bearings were measured. Positions of the thermocouples are shown in Fig. 2.

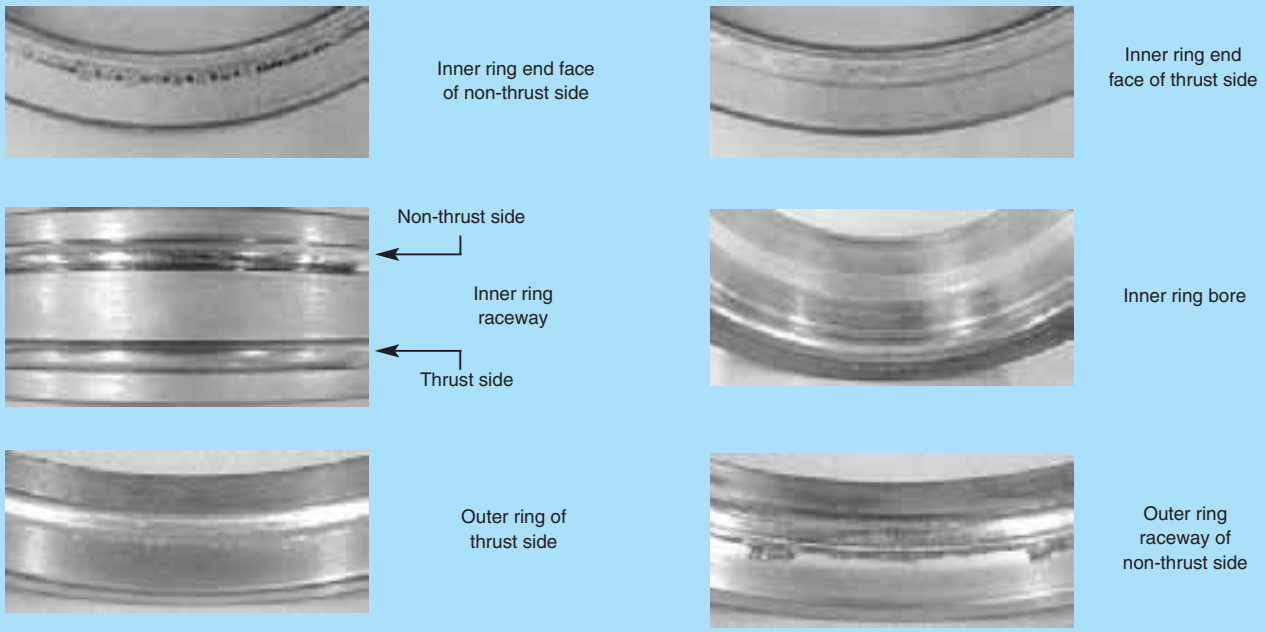

Fig. 4-1 Lower bearing after test

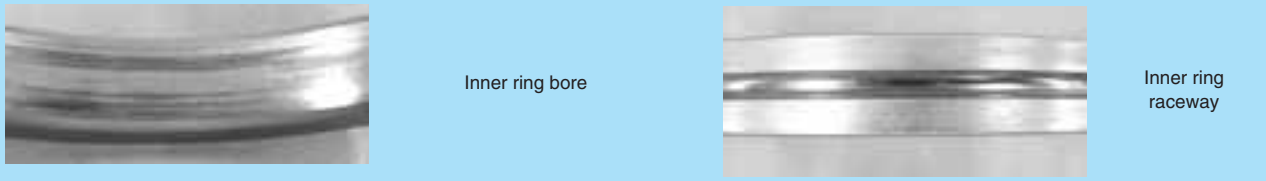

Fig. 4-2 Upper bearing after test

2.2 Test conditions and test bearings

Test conditions and the test bearings are listed in Table 1. Axial clearance of the lower side auxiliary bearing in the first test was designed to be smaller than that of a standard bearing.

2.3 Test results

(1) Shaft behavior

Axial displacement of the shaft, radial Lissajous, and changes in shaft rotation speed for the second and sixth trials respectively, are shown in Fig. 3. During the sixth trial, erratic bouncing of the shaft (vertical oscillation) was observed and found to be different from the type of bouncing that is normally found after delevitated coasting. Moderate movement of the shaft in an upward vertical direction was observed as well. Afterwards, the shaft continued to move upward until it could go no further.

(2) Bearing appearance

Fig. 4-1 and 4-2 show damage to the bearing from the sixth trial. Inner and outer ring wear traces of the lower non-thrust side bearing were observed. Axial clearance increased to about 0.065 mm. Contact between both ends and the shaft within the bore diameter of the upper and

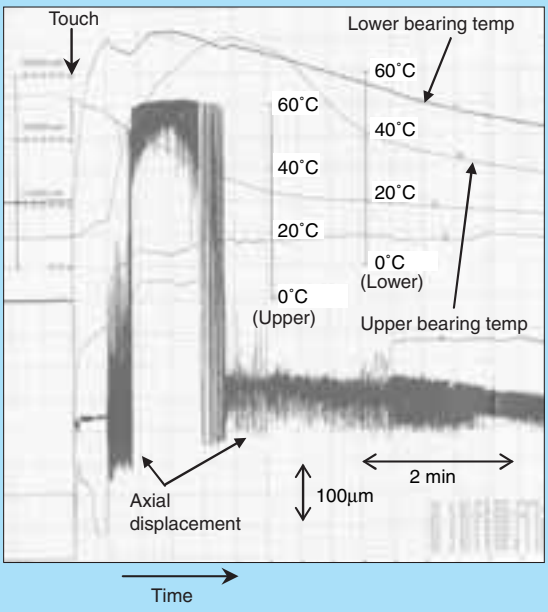

Fig. 5 Experimental results (Test No. 2)

lower bearings was strong. Slight contact was also observed on the surface at the point of contact of the non-thrust-side lower bearing.

(3) Temperature

Fig. 5 illustrates bearing temperature and axial displacement of the pump used in test No. 2. The sharp temperature rise of the upper bearing corresponds directly to when the shaft started bouncing, which continued for some time thereafter.

3. Examination

We examined the bouncing of the shaft and movement of the shaft in an upward vertical direction by estimating the load applied to the bearing based on the data regarding the shaft movement. Additionally, we investigated the relationship between these factors and damage of the non-thrust-side lower bearing.

3.1 Analysis

We determined that the shaft acts as a rotating element, moving in a gyroscopic manner, with a large amount of rotating energy, which is in unison with rectilinear movement. Accordingly, the coordinate system shown in Fig. 6 shows that the bearing was incapable of sustaining moment load, and force in the z-axis direction was ignored. An equation of the shaft movement can be expressed as follows:

$$m\frac{d^2r_G}{dt^2} = P_1 + P_2 \quad \cdots\cdots (1)$$

$$\frac{dH_G}{dt} = M_G \quad \cdots\cdots (2)$$

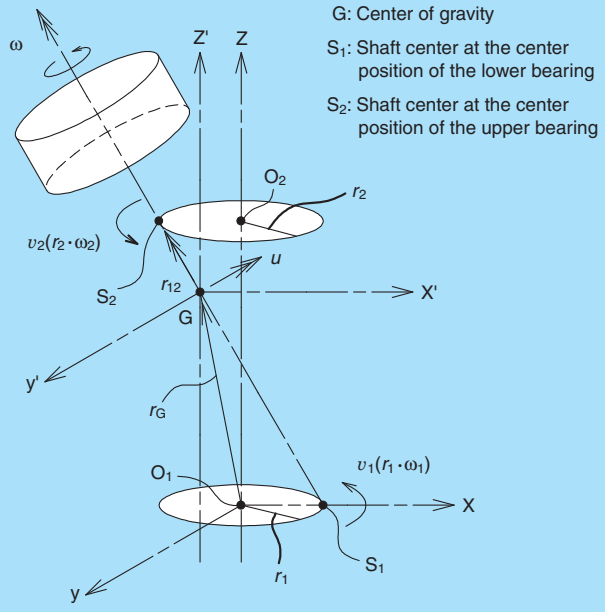

Fig. 6 Coordinate system

$$r_{1G} \times P_1 + r_{2G} \times P_2 = M_G \quad \cdots\cdots (3)$$

$$H_G = C\omega + Au \quad \cdots\cdots (4)$$

Here, u is a vector that crosses at right angles with ω and r_{12}, which is obtained from the following:

$$v_2 = v_1 + u \times r_{12} \quad \cdots\cdots (5)$$

$$u \cdot r_{12} = 0 \quad \cdots\cdots (6)$$

Explanation of symbols

- r_G: Position vector of center of gravity G from origin O
- r_{1G}: Vector from center of lower bearing S_1 to center of gravity
- r_{2G}: Vector from center of upper bearing S_2 to center of gravity
- r_{12}: Vector from shaft center S_1 to shaft center S_2
- P_1, P_2: Force applied from the bearing to the shaft at S_1 and S_2 respectively
- m: Mass of the rotating element
- M_G: Moment applied around G
- H_G: Angular momentum of G
- ω, u: Shaft center rotational angular velocity vector for r_{12} and orthogonal rotational angular velocity vector
- v_1, v_2: Tangential velocity vector at shaft center S_1 and S_2 respectively
- A, C: Moment of inertia

Therefore, when the data relating to r_1, r_2, ω_1, ω_2, and ω are obtained, radial loads P_1 and P_2, which are applicable to the bearing, can be determined. For the duration of calculation, r_1, r_2, ω_1, and ω_2 were regarded as being constant. The value of $d\omega/dt$ was obtained by differentiating the data of ω, which was necessary to calculate the torque component of the rotating axis.

3.2 Result of analysis

1) Torque (T)

Calculated torque (T) was added to the axial displacement data (See Fig. 3). Changes in T and axial displacement synchronized very well. This was especially true during bouncing, where torque increased abruptly.

2) Loads applied to the bearings (P_1 and P_2)

Whereas torque applied to the bearing (Tb) can be expressed as $T\mathrm{b} = u \cdot d\mathrm{m} \cdot \mathrm{P}$ (u : friction coefficient; dm: pitch circle diameter; P: radial load), by assuming the friction coefficients of the upper and lower bearings to be constant and equal, the sum of bearing torque was proportional to $T\mathrm{cal} = d\mathrm{m}_1 \cdot P_1 + d\mathrm{m}_2 \cdot P_2$. In Fig. 7, based on Tcal of point B1, and by using the maximum value of P_1 and P_2, the ratio of Tcal, including time lapse, was plotted.

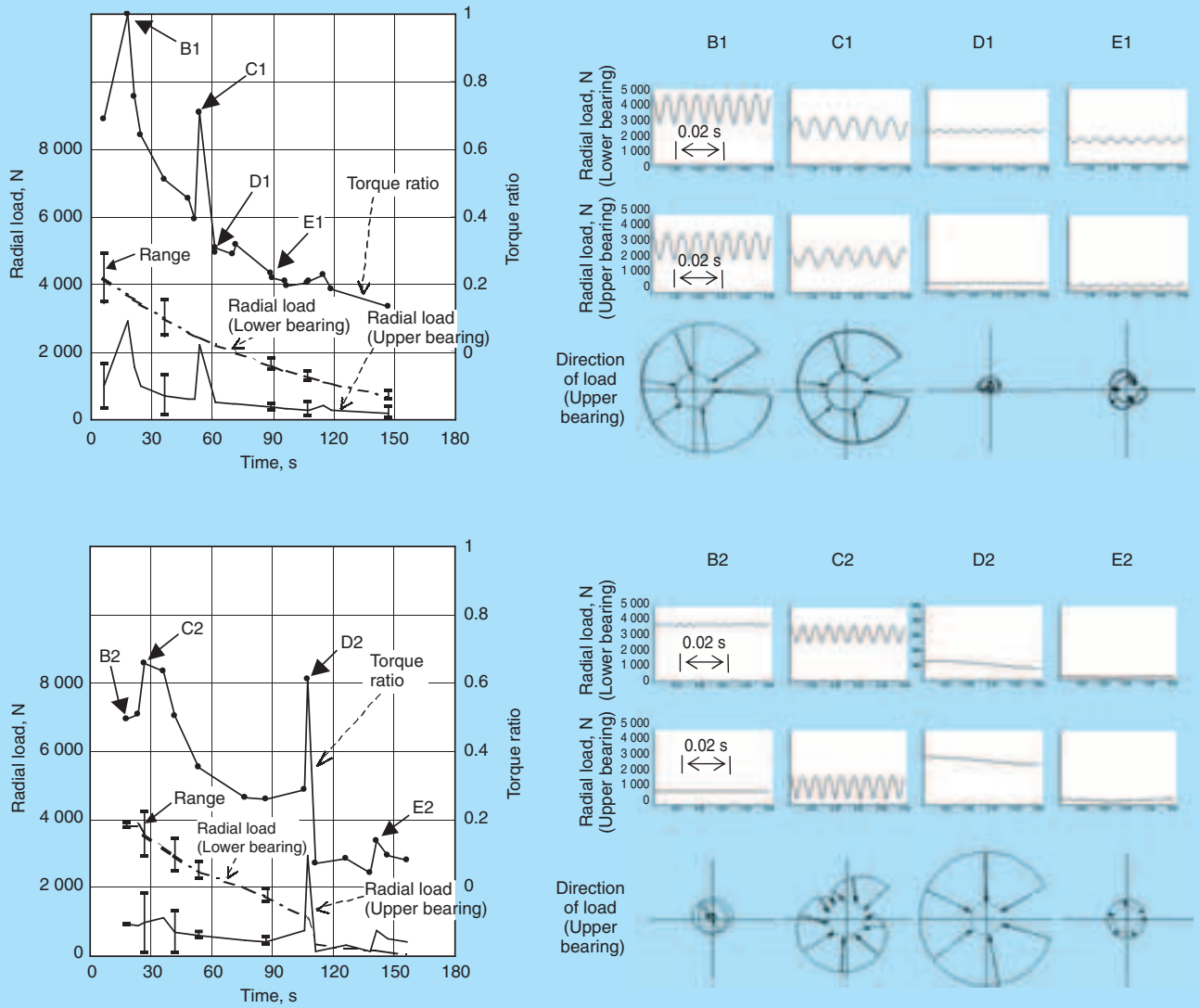

Here, 1 and 2 indicate the lower and upper bearings respectively. As a result, this data coincided with the tendency of torque (T) obtained from measured data. We are confident in the accuracy of P_1 and P_2, which was obtained from this analysis.

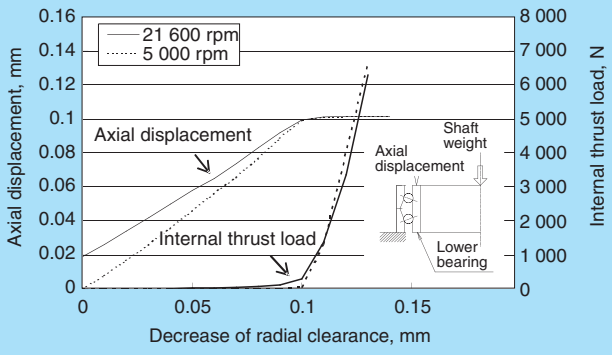

Fig. 8 Relationships between axial displacement, internal thrust load, and decrease of radial clearance

For about 150 seconds, we witnessed sudden bouncing and radial load being applied to the lower bearing, which is larger than that of the upper bearing (See Fig. 3 and 7). However, during bouncing, which occurred during D2, load applied to the upper bearing was momentarily larger than that of the lower bearing.

3) Axial displacement of the bearing

For the lower bearing, as internal clearance decreased due to heat generation, the shaft rose as shown in Fig. 8. As for negative clearance, the shaft eventually rose at half of the amount of axial clearance (0.1 mm in this case), maintained its position at that point, and generated a large internal load (See Fig. 8).

3.3 Cause of bouncing of the shaft and shaft rise

We determined that the "bounce force" was generated by frictional force generated through the large radial load acting between the shaft and the inner rings of the upper

bearing.

1) When bouncing occurred, the high whirl speed and radius of the shaft generated a large radial load, which was then applied to the upper bearing (See Fig. 7).
2) When whirl speed and radius of the shaft were large, tilting at the contact area of the bearing also became large. Relative sliding velocity between the shaft and the inner ring acted in the upper vertical direction at the contact point.
3) When bouncing occurred, the temperature of the upper bearing also rose, which explained the large radial load that was being applied to the upper bearing (See Fig. 5).
4) At the time of D2 (See Fig. 3), where it seemed that the lower non-thrust side bearings were damaged, the friction force was calculated from the loads applied to the upper bearing and lower bearings (See Fig. 7). For example, when we calculated the friction coefficient that occurred between the shaft and the inner ring of the bearing as 0.1 (MoS_2)[3], we were able to see generation of a thrust force that exceeded the weight of the shaft.

Alternatively, for moderate shaft rise, movement of the shaft was generated by the associated decrease of internal clearance of the bearing, which was due to heat generation that was caused by internal friction of the lower side bearing. The maximum rise of about 0.1 mm, as illustrated in Fig. 8, coincided with the measured value illustrated in Fig. 3.

Data from the sixth trial (See Fig. 3), after the rise of 0.1 mm, revealed a rise of about 0.075 mm that coincided with the increase of axial clearance of the lower bearing, which was caused by wear. Therefore, we concluded that shaft movement was a result of bearing wear.

3.4 Cause of bearing damage

Bouncing force was generated at the time of D2 as previously discussed. Meanwhile, Fig. 8 shows that the bearing internal load increased considerably due to negative internal clearance of the lower bearing. We believe that overlapping of internal load and thrust force amplified the load that was applied to the non-thrust side of the lower bearing, and thus caused wear, which ultimately resulted in bearing failure.

4. Conclusion

As a result of analysis of shaft behavior, the following information was attained:

(1) We were able to estimate the amount of load that was applied to the bearing. As a result, it was estimated that irregular shaft behavior including the bouncing phenomenon and bouncing force were related to frictional force generated through the large radial load acting between the shaft and the inner rings of the upper bearing.
(2) To ensure durability of the auxiliary landing bearings, in addition to minimizing the effect of heat generation of the bearing interiors and contact surface areas, the importance of the role that friction plays in restraining the generation of axial load was clarified.

References:

1) L. P. Tessier, "The development of an auxiliary bearing system for a flexible AMB supported hydrogen process compressor rotor," Proc. of MAG'97. Alexandria. USA. Aug. (1997)
2) A. Palmgren, "Grundlagen der Walzlagertechnik," (1964)
3) M. Mtasunaga and Y. Tutani "Handbook for solid lubrication" (1978)

Yukio Ooura

Sumio Sugita

Electrically Conductive Bearing Grease for Office Equipment

Hiroyuki Nakamura, NSK EUROPE LTD.
Touru Shoda, Bearing Technology Center

ABSTRACT

There is an increasing need for electrically conductive bearings for plain paper copiers (PPC) and laser beam printers (LBP). NSK has developed and started marketing bearings filled with either ECS or ECZ conductive bearing grease operating under normal temperatures of up to 100˚C. In addition, NSK has developed bearings filled with a new type of ECZ grease, which provides enhanced durability and reliability over former ECZ grease products. NSK's new ECZ grease has half of the volume resistivity (resistance change with time is small) of former ECZ grease products. At the same time, NSK has developed bearings filled with high-temperature conductivity grease (ECF grease), which has the same volume resistivity as the new ECZ, but provides greater durability under harsher operating temperatures up to 230˚C.

1. Introduction

There is an increasing need for electrically conductive bearings for plain paper copiers (PPCs) and laser beam printers (LBPs). Electrically conductive bearings enhance the cost performance of office equipment, and have an additional benefit of reducing electromagnetic waves that can interact with human beings, and may affect some electronic devices. In addition, print quality is assured.

Deep groove ball bearings used in office equipment are lubricated with special grease that contains carbon-black, which provides the bearing with electrical conductivity. This article introduces details regarding the performance of electrically conductive grease used with bearings for the photoreceptor drum assembly, developer roller, and paper transport assembly of PPCs and LBPs operating under normal temperatures of up to 100˚C. We will also cover grease performance of the bearings for the fuser unit, which operate under much higher temperatures up to 230˚C.

2. Electrically Conductive Grease for Normal Operating Temperatures Up to 100˚C

Whereas the photoreceptor drum assembly of a PPC or LBP is constantly being charged, correct grounding is necessary to permit electrical discharge. In some cases, proper electrical discharge is required for the developer roller and paper transport assembly to ensure print quality and as a measure against electromagnetic interference.

Generally, a grounding brush or plate spring is mounted to a shaft end as a measure against electrical discharge. For greater cost reductions, office equipment manufacturers are eliminating such devices as grounding systems, and are relying more on electrically conductive bearings to serve that function.

NSK has successfully marketed many kinds of electrically conductive grease such as ECS and ECZ grease for bearings used in photoreceptor drum assemblies and developer rollers. Our latest development is a bearing filled with new electrically conductive grease called New ECZ, which further enhances the durability and reliability of conventional ECZ grease.

2.1 Developmental goal

Development of the New ECZ grease focused on extending the duration of electrical conductivity of grease by minimizing the effects of grease degradation, which traditionally occurs over time. In order to achieve our goal, we had to reduce both the average electrical resistance and maximum electrical resistance to less than half of that of conventional ECZ grease. Other characteristics remained the same as those of conventional ECZ grease.

2.2 Brief summary of new ECZ grease

Special additives, which complement the excellent characteristics of conventional ECZ grease, were added to the grease to sustain a longer duration of electrical conductivity and durability.

2.3 Durability test results

Fig. 1 and 2, and Table 1 show the durability test results of a ball bearing (Bore diameter: 8 mm; outside diameter: 19 mm; and width: 6 mm), while Fig. 3 shows a wiring diagram of the electric circuit used for measuring electrical resistance. Both the average electrical resistance and maximum electrical resistance were less than half of those of conventional ECZ grease, which achieved our developmental goal. Remarkably, the maximum electrical resistance value of the New ECZ only slightly increased, and remained well within a range that was about 1/8th of that of conventional grease, even after operating for 3 200 hours. Furthermore, the test bearing remained free of any large peaks of electrical resistance.

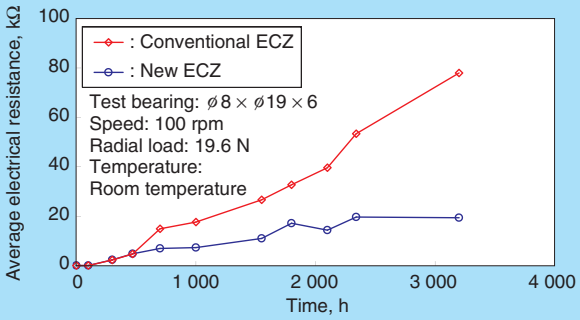

Fig. 1 Increase of average electrical resistance

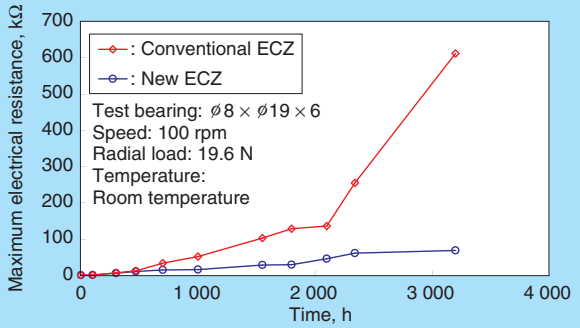

Fig. 2 Increase of maximum electrical resistance

Table 1. Electrical resistance after running

Unit: kΩ

	1 000 hours		3 200 hours	
	New ECZ	Conventional ECZ	New ECZ	Conventional ECZ
Average electrical resistance	7	18	19	79
Maximum electrical resistance	16	52	69	612

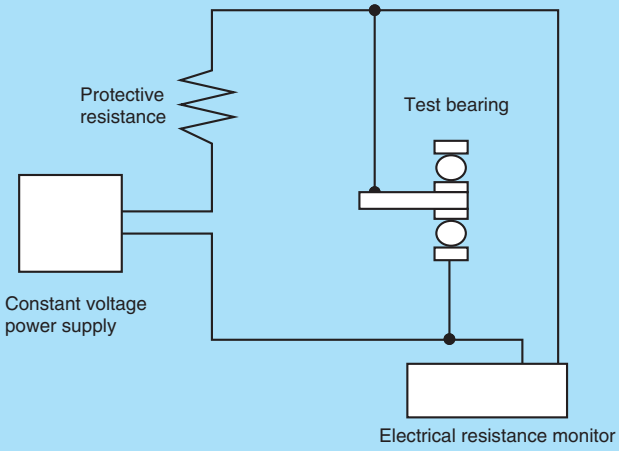

Fig. 3 Wiring diagram of electric circuit for measuring electrical resistance

3. Electrically Conductive Grease for High Operating Temperatures Up to 230˚C

Until recently, there was little demand for electrically conductive bearings for the fuser unit of a PPC or LBP. To meet current demand, NSK marketed bearings packed with electrically conductive grease called ECF, which was developed primarily for bearings operating under high temperature conditions.

3.1 Developmental goal

Electrical resistance after 1 000 hours and 3 000 hours of operation was almost the same as that of conventional ECZ grease.

Seizure resistance under high temperatures (200 to 300˚C) was almost the same as that of conventional KPM grease, which is a widely used and marketed fluorine-based grease for fuser units developed by NSK.

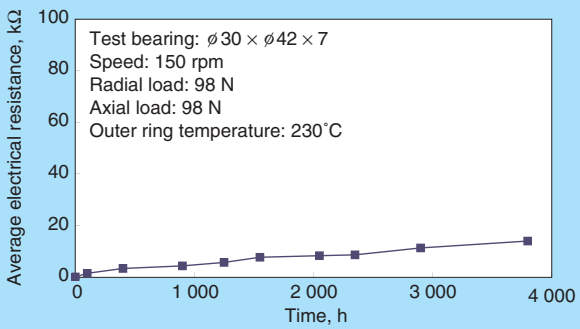

Fig. 4. Increase of average electrical resistance

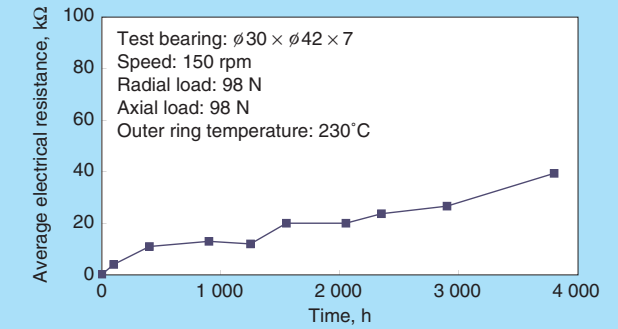

Fig. 5 Increase of maximum electrical resistance

3.2 Brief summary of ECF grease

ECF is a fluorine-based grease that consists of KPM grease combined with special carbon-black. The carbon-black provides electrical conductivity, while the KPM grease ensures excellent high-temperature durability. In addition, ECF grease contains a special additive for extending the duration of electrical conductivity by minimizing the effects of grease degradation.

3.3 Durability test results

Fig. 4 and 5 show the durability test results of a ball bearing (Bore diameter: 30 mm; outside diameter: 42 mm; and width: 7 mm). Fig. 3 shows the wiring diagram of the electric circuit used for measuring electrical resistance for this test bearing as well.

Bearing seizure test results are shown in Fig. 6.

Electrical resistance after 1 000 hours and 3 000 hours of operation was less than that of conventional ECZ grease, and was equal to or less than that of the New ECZ grease.

In addition, bearing seizure time was almost the same as that of KPM grease, which satisfactorily met our development goal.

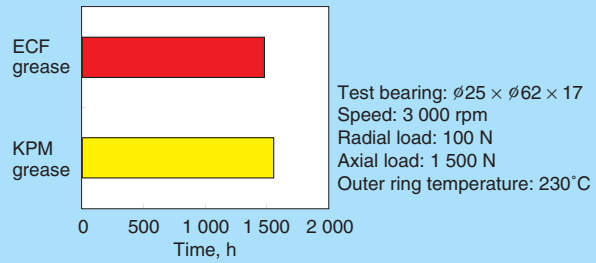

Fig. 6 Bearing seizure time

4. Conclusions

NSK's newly developed ECF and New ECZ electrically conductive grease products provide excellent electrical conductivity and stability at levels not available with conventional grease products. As office equipment manufacturers raise the performance standards of copiers and printers in the future, NSK will follow suit and continue to work on newly developed electrically conductive bearing grease to meet the demand for higher performance.

Hiroyuki Nakamura

Touru Shoda

ROBUST Series Ultra High-Speed Angular Contact Ball Bearings for Machine Tool Spindles

NSK developed the ROBUST series ultra high-speed angular contact ball bearings (Photo 1) for machine tool spindles. Machine tool manufacturers responded favorably to the ROBUST series as noted by its solid reputation in the marketplace, and continued mass-production. The success of this product lies in its ability to provide users with higher operating speeds and minimal thermal displacement of the spindle by ensuring low temperature rise of the bearing. Furthermore, we improved temperature stability robustness and seizure resistance, which are indispensable to motorized spindle applications.

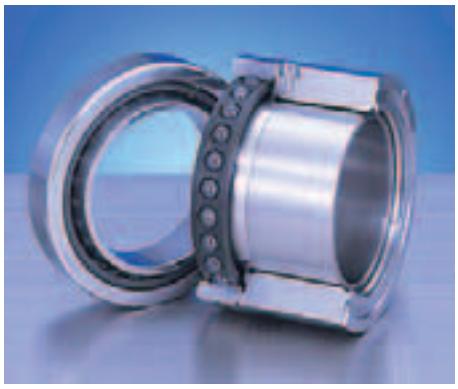

Photo 1 ROBUST series

1. Features

A. Better temperature stability "Robustness"

Under various cutting conditions or processing conditions with rotational fluctuations, changes in temperature of the main spindle can be quite extreme. Internal clearance of the bearing is reduced depending on differences in temperature between the inner and outer rings of the bearings. As the spindle temperature changes and the contact angle between the balls and inner and outer ring grooves rapidly changes, there is an increase of internal preload and PV value at the rolling contact points between the inner and outer ring grooves and balls.

However, fluctuations of internal load in the ROBUST series are extremely small, even under such harsh conditions as described above. This demonstrates how well the ROBUST series have been designed to ensure stable performance at all times under a variety of operating conditions.

B. Low heat generation

Differences in time delay properties against temperatures between the inner and outer rings surrounding heat transfer systems are also related to

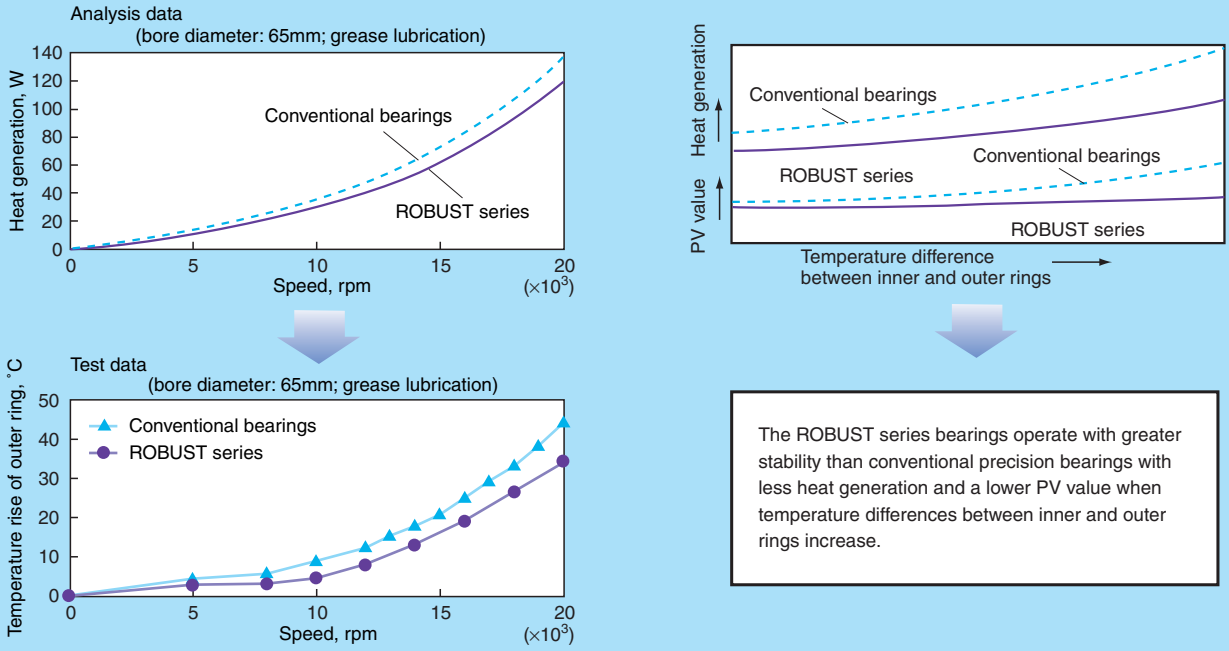

Fig. 1 Analysis and test data

differences in temperatures between the inner and outer rings during rapid acceleration. Improving heat displacement properties, which are particularly important to machine tools, is possible by minimizing the generation of heat by the bearing itself under such operating conditions.

Furthermore, high speed with grease lubrication is possible, which has less of an environmental impact. The low-heat generating design of the ROBUST series achieves a reduced temperature rise of about 20% compared to conventional bearings.

2. SHX Heat Resistant Material for X and XE Types

Our new SHX material is a heat resistant steel that has similar heat resistance performance to M50 steel, which is used for bearings on the main shaft of jet engines, where temperatures can reach as high as 300˚C. In further comparisons, SHX proves superior to M50 with respect to

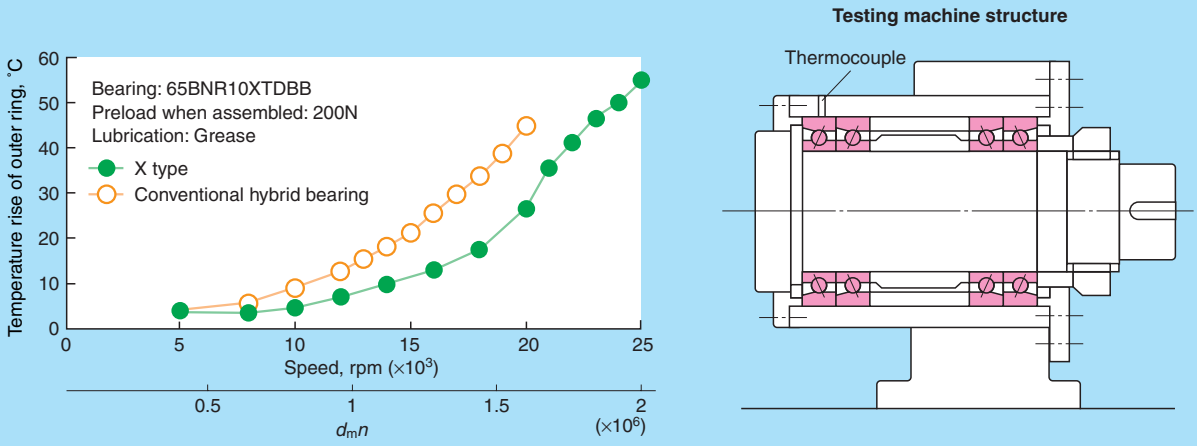

Fig. 2 Test data

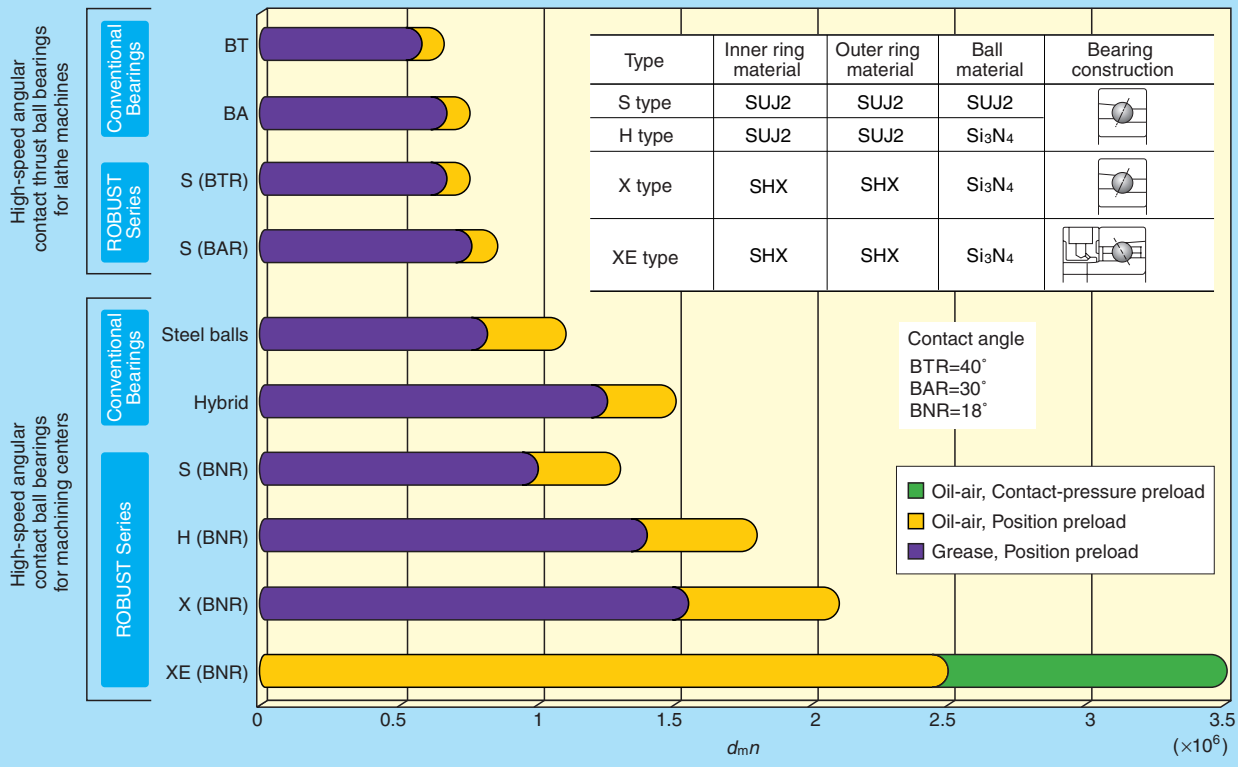

Fig. 3 ROBUST Series Ultra High-Speed Angular Contact Ball Bearings

wear resistance, seizure resistance, and durability. As such, SHX is most suitable for machine tool spindles, which must operate at high speeds under minimal lubrication conditions where it is also necessary to resist localized high temperatures in the Hertz contact area.

Fig. 2 illustrates temperature rise of a newly designed ROBUST series X-type hybrid angular contact ball bearing, which uses SHX material for the inner and outer rings, and grease lubrication. Temperature rise of the bearing is very low compared with that of conventional bearings, and remained stable under 25 000 rpm ($d_m n$ value: 2 million).

3. Structure and Range

There are four types of ROBUST series in which bearing structure and material differ for various operating conditions (Fig. 3).

4. Conclusions

Efforts to raise productivity through machine tool spindles that have higher speed and more rapid acceleration and deceleration capabilities are being pursued actively by machine tool operators.

NSK's ROBUST series reflect future bearing design to meet market demand.

For more information regarding the NSK ROBUST series, please refer to the following publications:

- Super Precision Bearings CAT. No. E1254 2003
- NSK Technical Journal, Motion & Control, No. 9 (October 2000)

Ultra-Precision NSK Linear Guides for Machine Tools—the HA Series

Recently, in response to improvements in the accuracy of machine tools and various machinery equipment, demand for enhanced motion accuracy of linear guideways have been growing. In pursuit of highly precise motion accuracy, the rolling linear guides such as NSK linear guides that require infinite re-circulation of balls are faced with a slight linear motion error caused by minute vibration due to the balls that are going in and out of the load zones. Hence, linear air bearings and sliding linear guideways have been used for application requiring extremely high accuracy.

The linear air bearing is, however, difficult to control and is very expensive, while the sliding linear guideway is inferior at high operating speeds, and requires intensive maintenance.

This is the reason why we have pushed for improvements in the motion accuracy of NSK linear guides.

We are introducing here NSK HA (High Accuracy) series ultra-precision linear guides (Photo 1) that have minimized the slight linear motion error.

1. Features

The HA series is a newly developed product based on NSK LA series linear guides for machine tools, and incorporates the features required for highly accurate linear positioning.

(1) Highly precise motion accuracy
Vibration caused by ball passage is reduced by an ultra-long ball slide and optimum design of the ball re-circulation.

(2) High stiffness and high load capacity
An increase in the number of balls ensures high stiffness and high load capacity.

(3) Superior dust resistance
The inner seal, which comes as standard equipment, improves durability and accuracy life under contaminated operating conditions.

(4) Improved straightness of the rail mounting
- For further enhancing straightness of the rail mounting, the pitch of rail fixing bolt holes have been reduced to half of the conventional pitch.
- The depth of the counterbore of the mounting bolt hole has been extended, thus reducing the pitching error of the ball the raceways of the rail, caused by compression of the bottom wall of rail, resulting from bolt tightening.

Comparison data of vibration caused by ball passage of the HA series and conventional linear guides using the same table base is shown in Fig. 1. At the 500 mm overhang point, from the center of the table in the direction of motion axis, the vibration caused by ball passage in vertical directions was measured.

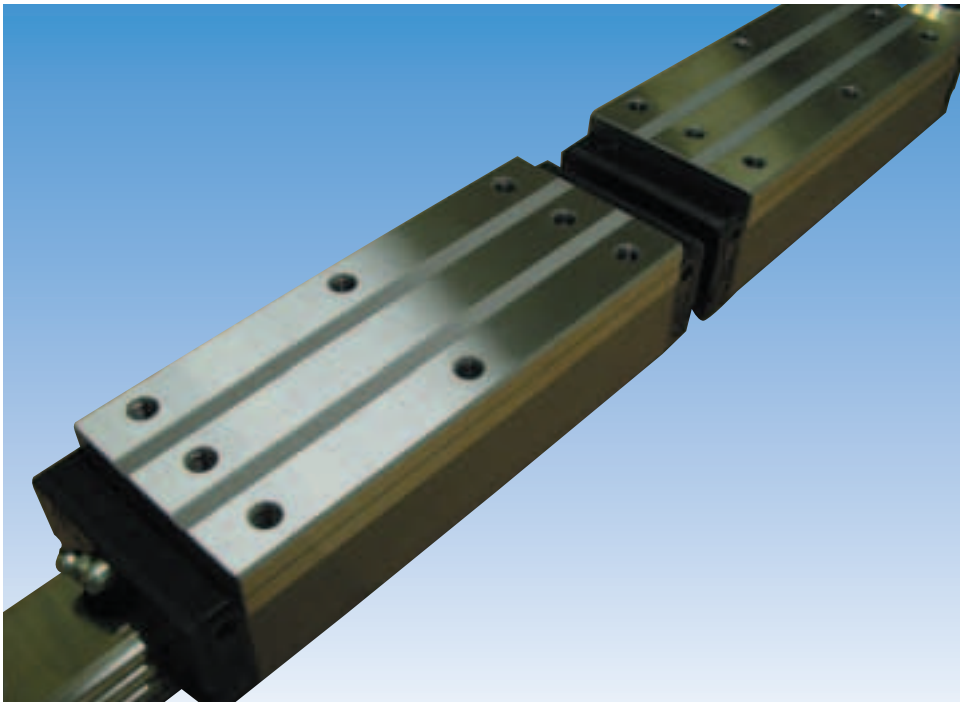

Photo 1 HA series

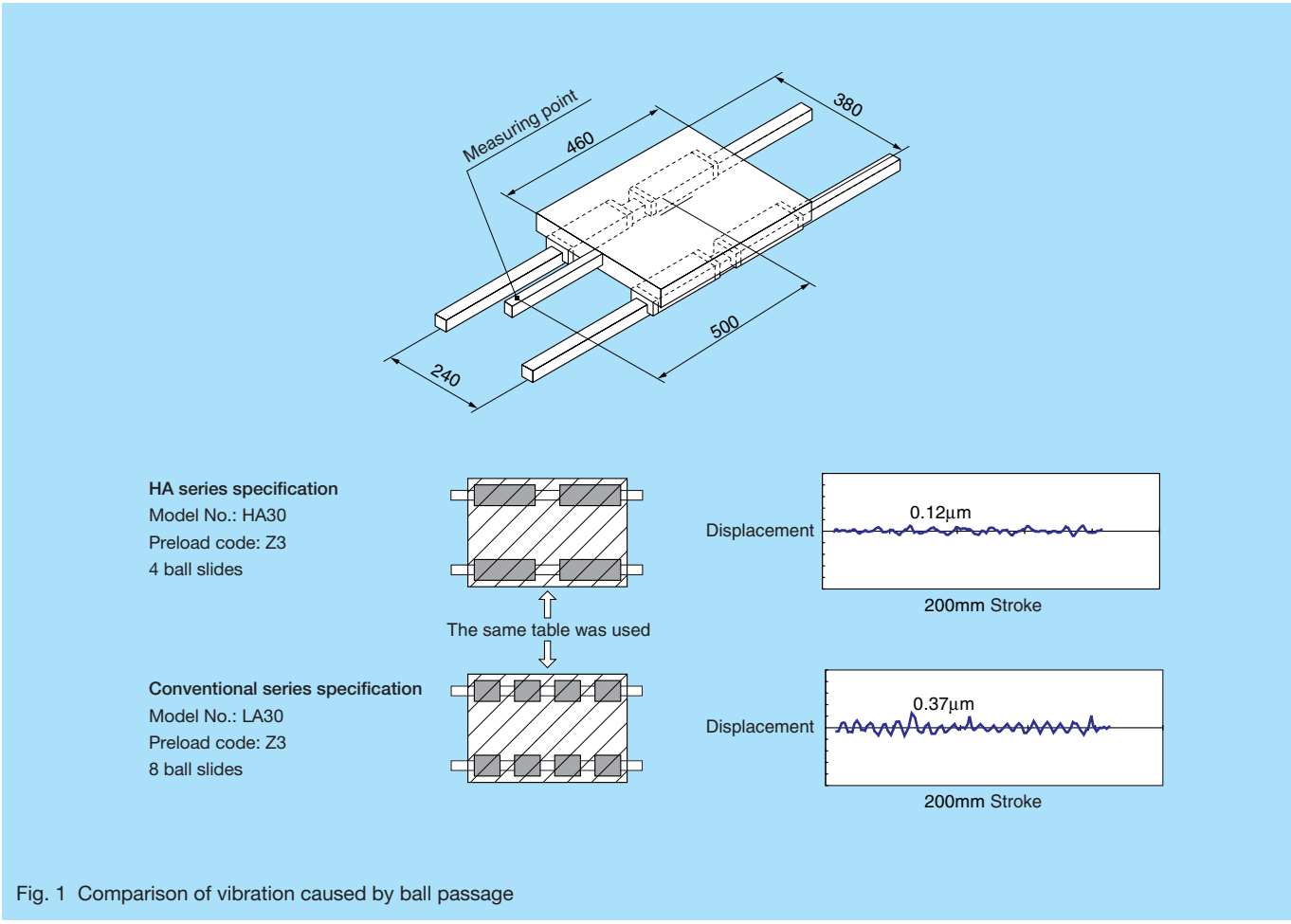

Fig. 1 Comparison of vibration caused by ball passage

Table 1 Model number and type of ball slide

Model No.	Type of ball slide		
	AN: Square type	AL: Low square type	EM: Flanged type
HA25	○	—	○
HA30	○	—	○
HA35	○	○	○
HA45	○	○	○
HA55	○	○	○

2. Specifications

The model numbers and types of HA series ball slides are shown in Table 1.

Boundary dimensions of the square type of ball slide (AN) are shown in Table 2 as an example.

(1) Types and dimension
Ball slide length has been doubled in comparison to the standard length of the LA series. Mounting tap holes of the flanged type ball slide can be also used as bore holes, which makes it possible to secure the ball slide from either side of the ball slide.

(2) Accuracy and preload
Accuracy grades conform to LA series.
Medium preload (Z3) and slight preload (Z1) are available.

(3) Options
The NSK K1® lubrication unit can be equipped for extended maintenance-free performance.

3. Applications

The high-precision motion accuracy of the HA series is ideal for applications such as machining centers, precision lathes, and grinding machines. Furthermore, the low friction and high stiffness of this series are well suited for electric discharge machines.

4. Conclusion

In response to market demand for greater precision, NSK has developed and marketed a new type of linear guide that ensures high-precision motion accuracy at levels unachievable by conventional linear guides. We will apply our developments to other series and develop high precision linear guides in all industrial fields in the future.

Table 2 Dimensions (AN type)

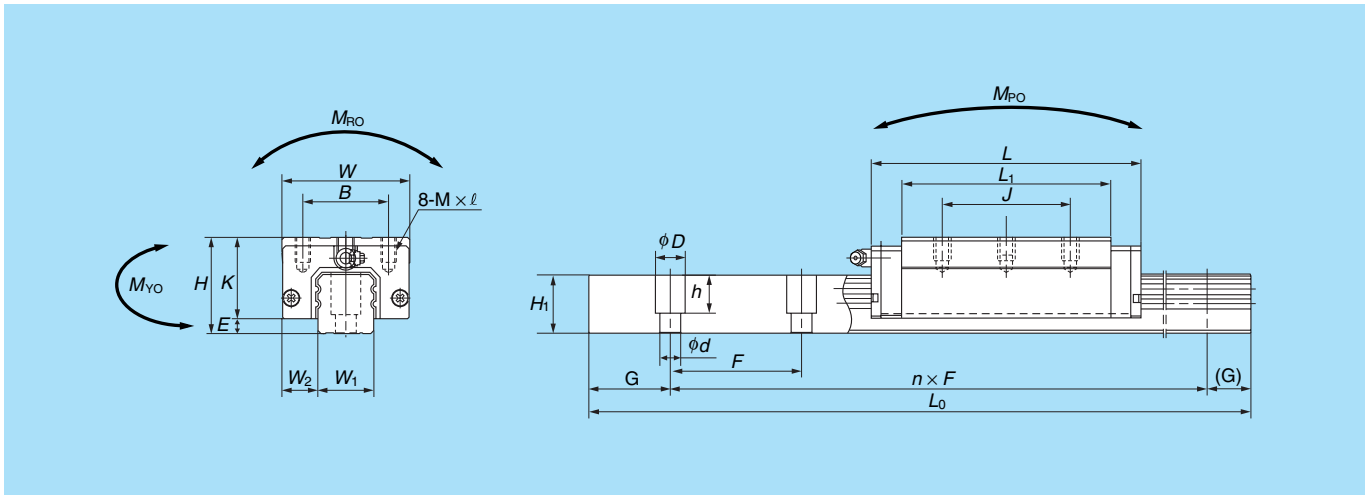

Model No.	Assembly			Ball slide						
	Height			Width	Length	Mounting tap hole				
	H	E	W_2	W	L	B	J	M × Pitch × ℓ	L_1	K
HA25AN	40	5.5	12.5	48	147.8	35	100	M6 × 1.0 × 10	126	34.5
HA30AN	45	7.5	16	60	177.2	40	120	M8 × 1.25 × 11	149	37.5
HA35AN	55	7.5	18	70	203.6	50	140	M8 × 1.25 × 12	173	47.5
HA45AN	70	10	20.5	86	233.4	60	160	M10 × 1.5 × 16	197	60
HA55AN	80	12	23.5	100	284.4	75	206	M12 × 1.75 × 18	245	68

Model No.	Rail						Basic load rating				
	Width	Height	Pitch	Mounting bolt hole	G	Maximum length	Dynamic	Static	Static moment (N·m)		
	W_1	H_1	F^*	$d \times D \times h^*$	(recommended)	$L_{0\,max}$	C	C_0	M_{RO}	M_{PO}	M_{YO}
HA25	23	22	30/60	7 × 11 × 16.5/9	20	3 960	54 000	115 000	670	2 060	2 060
HA30	28	28	40/80	9 × 14 × 21/12	20	4 000	79 500	166 000	1 140	3 550	3 550
HA35	34	30.8	40/80	9 × 14 × 23.5/12	20	4 000	111 000	226 000	1 950	5 650	5 650
HA45	45	36	52.5/105	14 × 20 × 27/17	22.5	3 990	147 000	295 000	3 700	8 450	8 450
HA55	53	43.2	60/120	16 × 23 × 32.5/20	30	3 960	232 000	445 000	6 500	15 400	15 400

*Pitch of rail mounting bolt hole F and size of rail mounting bolt hole h are selectable.

Clean Support Units for Ball Screws

Taking advantage of NSK's advanced bearing technology, we have been developing support units for ball screws as optional accessories for over 20 years. To ensure that our products meet low dust generation requirements of the semiconductor industry, we have developed a new series of clean support units (Photo 1) for clean environments. Our new support units include special angular contact bearings with newly developed non-contact seals for light load applications and for small equipment.

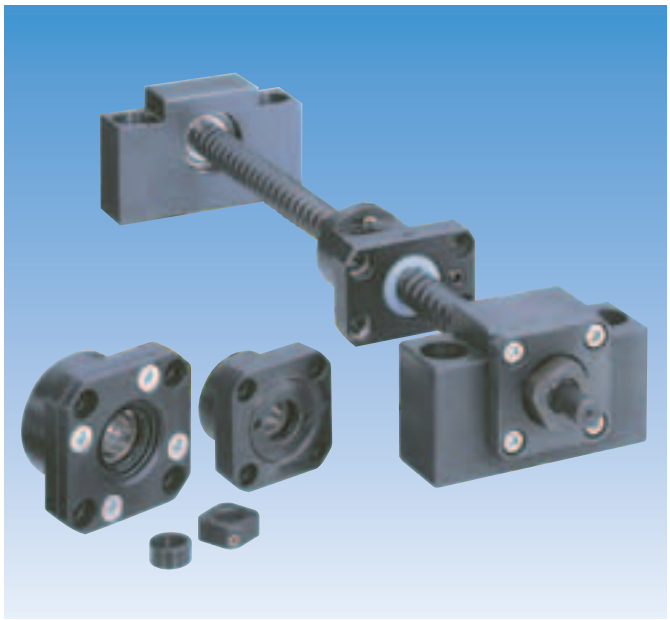

Photo 1 Clean support units

1. Specifications and Performance

Table 1 provides a convenient comparison of our newly developed clean support unit and conventional support unit.

Table 2 lists performance details of NSK's new clean support unit. Mounting dimensions are the same as conventional support units for light load applications and small equipment.

Table 1 Comparison of support units

	Clean support unit	Conventional support unit
Unit reference number	WBK∗∗-∗∗C	WBK∗∗-∗∗A
Fixed side bearing	New type angular contact ball bearing with non-contact seal	Standard angular contact ball bearing without seal
Grease	LG2	PS2
Housing, cover, and locknut	Carbon steel, and low temperature chrome plating	Carbon steel, and black oxide coating
Spacer	Carbon steel, and low temperature chrome plating	Carbon steel with no surface treatment
Bolt and snap ring	Stainless steel	Carbon steel
Seal	Nitrile rubber	Nitrile rubber

Table 2 Performance details

Support unit reference number	Fixed support side unit					Simple support side unit		
	Bearing bore (mm)	Axial direction			Maximum starting torque (N·cm)	Bearing bore (mm)	Bearing number	Radial direction
		Basic dynamic load rating (N)	Limit load (N)	Rigidity (N/μm)				Basic dynamic load rating (N)
WBK08	8	3 100	1 100	35	0.5	6	606VV	2 250
WBK10	10	4 250	1 350	50	1.1	8	608VV	3 300
WBK12	12	4 700	2 450	55	1.2	10	6000VV	4 550
WBK15	15	5 100	2 750	65	1.3	15	6002VV	5 600

2. Features

1) Low dust generation
Clean support units are lubricated with NSK LG2 grease, which has been well accepted for use in clean-room applications. Using LG2 grease, we were able to reduce the amount of dust generation to about one-tenth (Fig. 1) of that found in conventional support units.

2) Low torque
Torque performance over load capacity was the primary focus in developing the angular contact ball bearings used in fixed end support units for light load applications. As a result, dynamic torque was reduced by almost 50 percent compared to conventional support units with the added benefit of lower dynamic torque performance (Fig. 2).

3) High corrosion resistance
Superior corrosion resistance is achieved by the use of stainless steel components and low temperature chrome plating.
4) Quick delivery
Stock levels of the new clean support units, both fixed support side units (square type and round type) and simple support side units (square type), are well maintained to the same degree of the conventional support units for shorter lead times.

3. Applications

NSK's new clean support units are designed for light load applications, including semiconductor manufacturing equipment, medical equipment, clean room equipment, and measuring instruments. We highly recommend our new clean support units for use with ball screws or linear guides operating in clean environments.

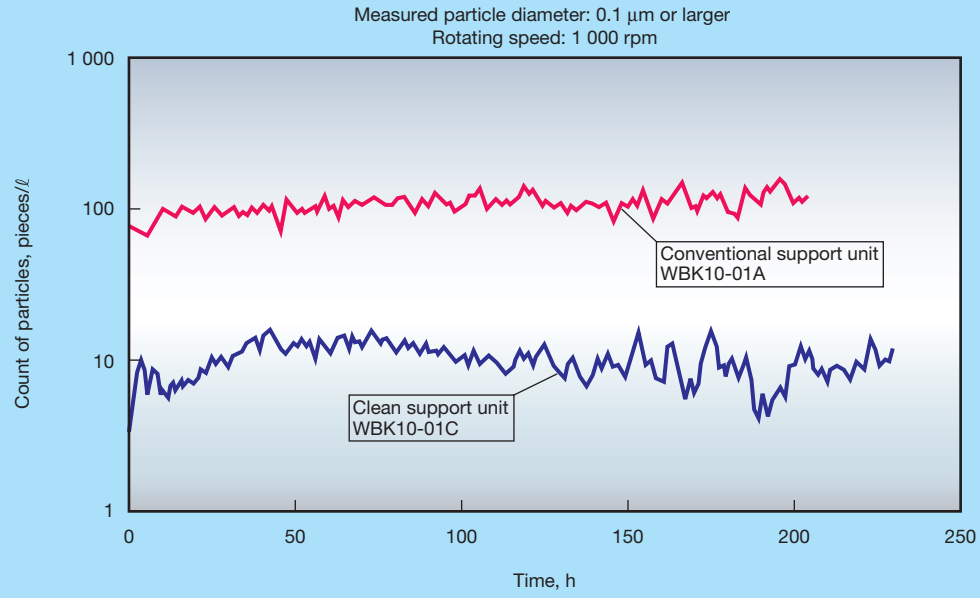

Fig. 1 Dust generation

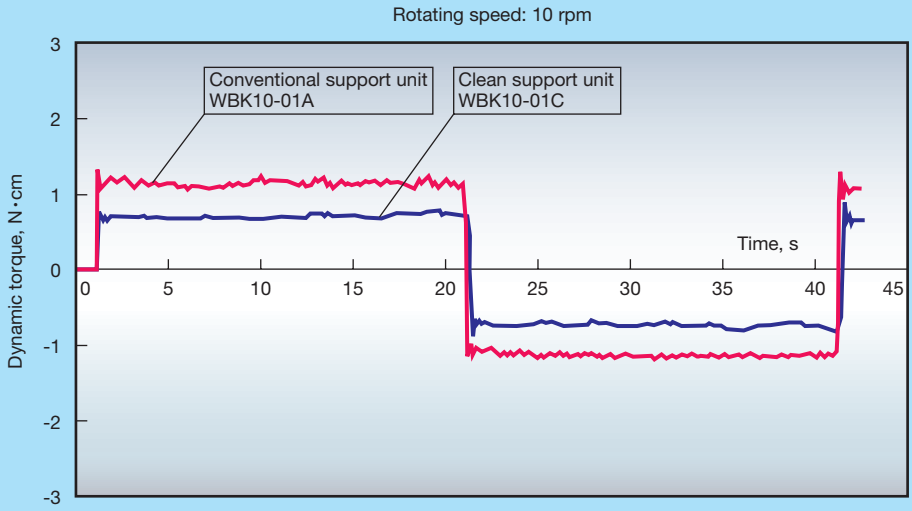

Fig. 2 Dynamic torque

Worldwide Sales Offices and Manufacturing Plants

NSK LTD.–HEADQUARTERS, TOKYO, JAPAN www.nsk.com
OVERSEAS CS DEPARTMENT / ASIA BUSINESS STRATEGIC DIVISION-HEADQUARTERS
Nissei Bldg., 6-3, Ohsaki 1-chome, Shinagawa-ku, Tokyo 141-8560, Japan
P: 03-3779-7680 F: 03-3779-7433 C: 81
Nissei Bldg., 6-3, Ohsaki 1-chome, Shinagawa-ku, Tokyo 141-8560, Japan
P: 03-3779-7121 F: 03-3779-7433 C: 81

Africa

South Africa:

NSK SOUTH AFRICA (PTY) LTD.
JOHANNESBURG 25 Galaxy Avenue, Linbro Business Park, Sandton, 2146, Gauteng, P.O. Box 1157, Kelvim, 2054 South Africa
P: (011) 458 3600 F: (011) 458 3608 C: 27

Asia and Oceania

Australia:

NSK AUSTRALIA PTY. LTD. www.nskaustralia.com.au
MELBOURNE 11 Dalmore Drive, Scoresby, Victoria 3179, Australia
P: (03) 9764-8302 F: (03) 9764-8304 C: 61
SYDNEY Unit 1, Riverside Centre, 24-28 River Road West, Parramatta, N.S.W. 2150, Australia
P: 02-9893-8322 F: 02-9893-8406 C: 61
BRISBANE 91 Wellington Road, East Brisbane, Queensland 4169, Australia
P: 07-3393-1388 F: 07-3393-1236 C: 61
ADELAIDE 64 Greenhill Road, Wayville, South Australia 5034, Australia
P: 08-8373-4811 F: 08-8373-1053 C: 61
PERTH Unit 4, 36 Port Kembla Drive, Bibra Lake, Western Australia 6163, Australia
P: 089-434-1311 F: 089-434-1318 C: 61

China:

NSK HONG KONG LTD.
HONG KONG Room 512, Wing On Plaza, Tsim Sha Tsui East, Kowloon, Hong Kong
P: 2739-9933 F: 2739-9323 C: 852

KUNSHAN NSK CO., LTD.
KUNSHAN 258 South Huang Pu Jiang Rd Kunshan E&T Development Zone Jiang Su 215335, China
P: 0512-5771-5654 F: 0512-5771-5689 C: 86

GUIZHOU HS NSK BEARINGS CO., LTD.
ANSHUN Dongjiao, Anshun, Guizhou, 561000, China
P: 0853-3521505 F: 0853-3522722 C: 86

NSK (SHANGHAI) TRADING CO., LTD.
SHANGHAI Room 826, No.1 Ji Long Road, Wai Gao Qiao Free Trade Zone, Shanghai, China
P: 021-62099051 F: 021-62099053 C: 86

NSK REPRESENTATIVE OFFICES www.nsk.com.cn
BEIJING Room 1001, Beijing Fortune Bldg., 5 Dong san Huan Bei Lu, Chao Yang District, Beijing, 100004, China
P: 010-6590-8161 F: 010-6590-8166 C: 86
SHANGHAI Room 1005, Shanghai International Trade Center 2200 Yan An Road (w.), Shanghai, 200336, China
P: 21-6209-9051 F: 21-6209-9053 C: 86
GUANGZHOU Room 2701-02, Guangzhou International Electronics Tower 403, Huan Shi Rd East, Guangzhou, 510095, China
P: 020-8732-0583 F: 020-8732-0574 C: 86
ANSHUN Dongjiao, Anshun, Guizhou, 561000, China
P: 0853-3522522 F: 0853-3522552 C: 86

NSK (CHINA) INVESTMENT CO., LTD
SHANGHAI Room 1007, Shanghai International Trade Center 2201 Yan An Road (W.) Shanghai, 200336, China
P: 021-62099051 F: 021-62099053 C: 86

India:

RANE NASTECH LTD.
CHENNAI 14, Rajagopalan Salai, Vallancherry Guduvancherry, Pin-603 202, India
P: 044-2433-4732, 044-2434-3036, 3067 F: 044-2433-4733 C: 91

NSK REPRESENTATIVE OFFICE
CHENNAI 2A, First Street, Cenotaph Road, Chennai, 600 018, India
P: 044-2433-4732, 044-2434-3066, 3067 F: 044-2433-4733 C: 91

Indonesia:

PT. NSK BEARINGS MANUFACTURING INDONESIA
JAKARTA PLANT Blok M-4, Kawasan Berikat, MM2100, Industrial Town, Cikarang Barat, Bekasi 17520, Jawa Barat, Indonesia
P: 021-898-0155 F: 021-898-0156, 021-898-0183 C: 62

PT. NSK INDONESIA
JAKARTA SummitmasII 6th Floor, Jl. Jend. Sudirman Kav. 61-62, Jakarta 12190 Indonesia
P: 021-252-3458 F: 021-252-3223 C: 62

Korea:

NSK KOREA CO., LTD. www.nsk.co.kr
SEOUL 9F (West Wing) Posco Center 892, Deachi 4 Dong Kangnam-Ku, Seoul, Korea
P: 02-3287-0300 F: 02-3287-0345, 0445 C: 82
CHANGWON PLANT 60, Songsan-Dong, Changwon, Kyungsangnam-Do, Korea
P: 055-287-6001 F: 055-285-9982 C: 82

Malaysia:

NSK BEARINGS (MALAYSIA) SDN. BHD.
KUALA LUMPUR 1001, Level 10, Uptown.2, 2 Jalan SS21/37, Damansara Uptown, 47400 Petaling Jaya, Selangor Darul Ehsan, Malaysia
P: 03-77223373 F: 03-77285543, 77287450 C: 60
PRAI 10, Lengkok Kikik 1, Taman Inderawasih, 13600 Prai, Penang, Malaysia
P: 04-3991763 F: 04-3991830 C: 60
JOHOR BAHRU Ground Floor, No. 27, Jalan Bakawali 50, Taman Johor Jaya, 81100 Johor Bahru, Johor, Malaysia
P: 07-3546290 F: 07-3546291 C: 60
KOTA KINABALU Lot 10, Lrg. Kurma 4, Likas Ind. Centre, 5 1/2Miles, Jalan Tuaran, 88450 Inanam Sabah, Malaysia
P: 088-421260 F: 088-421261 C: 60

NSK MICRO PRECISION (M) SDN. BHD.
MALAYSIA PLANT No.43 Jalan Taming Dua,Taman Taming Jaya, 43300 Balakong, Selangor Darul Ehsan, Malaysia
P: 03-961-6288 F: 03-961-6488 C: 60

New Zealand:

NSK NEW ZEALAND LTD. www.nsk-rhp.co.nz
AUCKLAND 3 Te Apunga Place Mt. Wellington, Auckland, New Zealand
P: (09) 276-4992 F: (09) 276-4082 C: 64

Philippines:

NSK REPRESENTATIVE OFFICE
MANILA Unit 910 Philippine AXA Life Centre, 1286 Seno Gil Puyat Avenue, Makati City 1200, Metro Manila, Philippines
P: 02-759-6246 F: 02-759-6249 C: 63

Singapore:

NSK INTERNATIONAL (SINGAPORE) PTE LTD.
SINGAPORE 2 Toh Guan Road East #02-02 Singapore 608837
P: (65) 6273 0357 F: (65) 6275 8937 C: 65

NSK SINGAPORE (PTE) LTD.
SINGAPORE 2 Toh Guan Road East #02-03 Singapore 608837
P: (65) 6278 1711 F: (65) 6273 0253 T: RS24058 C: 65

Taiwan:

TAIWAN NSK PRECISION CO., LTD.
TAIPEI 9th Fl., 34, Chung Shan N. Rd., Sec. 3, Taipei, Taiwan R.O.C.
P: 02-2591-0656 F: 02-2597-3101 C: 886
TAICHUNG 107-6, SEC. 3, Wenxin Rd., Taichung, Taiwan R.O.C.
P: 04-2311-7978 F: 04-2311-2627 C: 886

Thailand:

NSK BEARINGS (THAILAND) CO., LTD.
BANGKOK 25th Floor RS Tower, 121/76-77 Rachadaphisek Road, Dindaeng, Bangkok 10320, Thailand
P: 02-6412150~58 F: 02-6412161 C: 66

NSK BEARINGS MANUFACTURING (THAILAND) CO., LTD.
CHONBURI 700/430 Moo 7, Amata Nakorn Industrial Estate T. Donhualor, A. Muangchounburi, Chonburi 20000 Thailand
P: (038) 454010~454016 F: (038) 454017, 454020 C: 66

SIAM NSK STEERING SYSTEMS CO., LTD.
CHACHOENGSAO 90 Moo 9, Wellgrow Industrial Estate, Km. 36 Bangna-Trad Road, Bangwao, Bangpakong, Chachoengsao 24180, Thailand
P: (038) 522-343~350 F: 038-522-351 C: 66

Europe

NSK EUROPE LTD. (EUROPEAN HEADQUARTERS) www.eu.nsk.com
MAIDENHEAD, UK Belmont Place, Belmont Road, Maidenhead, Berkshire SL6 6TB U.K.
P: 01628-509800 F: 01628-509808 C: 44

France:

NSK FRANCE S.A.
PARIS Quartier de l'Europe, 2 Rue Georges Guynemer, 78283 Guyancourt Cedex, France
P: 01 30 57 39 39 F: 01 30 57 00 01 C: 33

Germany:

NSK DEUTSCHLAND GMBH
DÜSSELDORF Harkortstrasse 15, 40880 Ratingen, Germany
P: 02102-481-0 F: 02102-481-2290 C: 49
STUTTGART Sielminger Str. 65, 70771 Leinfelden-Echterdingen, Germany
P: 0711-79082-0 F: 0711-79082-289 C: 49
LEIPZIG Zschortauer Str. 76, 04129 Leipzig, Germany
P: 0341-5631241 F: 0341-5631243 C: 49

NSK PRECISION EUROPE GMBH
DÜSSELDORF Harkortstrasse 15, 40880 Ratingen, Germany
P: 02102-481-0 F: 02102-481-2290 C: 49

NSK STEERING SYSTEMS EUROPE LTD.
STUTTGART Sielminger Strasse 65 D-70771 Leinfelden-Echterdingen, Germany
P: 0771-79082-277 F: 0771-79082-289 C: 49

NEUWEG FERTIGUNG GMBH
CORPORATE / OFFICE/PLANT Ehinger Strasse 5, D-89593 Munderkingen, Germany
P: 07393-540 F: 07393-3732 C: 49

Italy:

NSK ITALIA S.P.A.
MILANO Via Garibaldi, 215 20024 Garbagnate Milanese (MI), Italy
P: 02-99-5-19-1 F: 02-990-25-778, 02-990-28-373 C: 39

INDUSTRIA CUSCINETTI SPA
TORINO Via Giotto 4, 10080, S. Benigno C. se, Torino, Italy
P: 0119824811 F: 0119880284 C: 39

Netherlands:

NSK EUROPEAN DISTRIBUTION CENTRE B.V.
De Kroonstraat 38, 5048 AP Tilburg, Nederland
P: 013-4647647 F: 013-4647648 C: 31

Poland:

NSK EUROPE LTD. WARSAW LIAISON OFFICE
WARSAW LIAISON OFFICE Przedstawicielstowo w Warszawie, ul. Migdalowa 4 lok. 73, 02-796 Warsaw, Poland
P: 022-645-1525, 1526 F: 022-645-1529 C: 48

NSK ISKRA S.A.
CORPORATE / OFFICE/PLANT UL. Jagiellonska 109, 25-734 Kielce, Poland
P: 041-366-5001 F: 041-366-5008 C: 48

NSK EUROPEAN TECHNOLOGY CENTER, POLAND OFFICE
UL. Jagiellonska 109, 25-734 Kielce, Poland
P: 041-366-5812 F: 041-366-5206 C: 48

Spain:

NSK SPAIN S.A.
BARCELONA Calle de la Hidráulica, 5, P.I. "La Ferrería" 08110 Montcada i Reixac (Barcelona), Spain
P: 093-575-4041 F: 093-575-0520 C: 34

Turkey:

NSK BEARINGS MIDDLE EAST TRADING CO., LTD.
ISTANBUL Yali Mahallesi, Fevzi Cakmak Caddesi, Caglar Apartman No.11/4, Maltepe 81530, Istanbul, Turkey
P: 0216-442-7106 F: 0216-305-5505 C: 90

United Kingdom:

NSK BEARINGS EUROPE LTD.
PETERLEE PLANT 3 Brindley Road, South West Industrial Estate, Peterlee, Co. Durham, SR8 2JD U.K.
P: 0191-586-6111 F: 0191-586-3482 C: 44
Davey Drive, North West Industrial Estate, Peterlee, Co. Durham, SR8 2PW U.K.
P: 0191-518-0777 F: 0191-518-0303 C: 44
NEWARK PLANT Northern Road, Newark, Nottinghamshire, NG24 2JF U.K.
P: 01636-605123 F: 01636-642083 C: 44

NSK EUROPEAN TECHNOLOGY CENTRE
NEWARK, UK Northern Road, Newark, Notts, NG24 2JF U.K.
P: 01636-605123 F: 01636-643241 C: 44

NSK UK LTD.
NEWARK Northern Road, Newark, Nottinghamshire, NG24 2JF U.K.
P: 01636-605123 F: 01636-643050 C: 44

NSK STEERING SYSTEMS EUROPE LTD.
CORPORATE / OFFICE / PETERLEE / PLANT Silverstone Drive, Rowiey's Green, Coventry, CV6 6PA U.K.
P: 024-76-588588 F: 024-76-588599 C: 44
6/7 Doxford Drive, South West Industrial Estate, Peterlee, Co. Durham, SR8 2RL U.K.
P: 0191-518-6400 F: 0191-518-6421 C: 44

North and South America

NSK AMERICAS, INC. (AMERICAN HEADQUARTERS)
ANN ARBOR, USA 4200 Goss Road, Ann Arbor, MI 48105-2703
P: 734-913-7500 F: 734-913-7511 C: 1

Argentina:

NSK ARGENTINA SRL
BUENOS AIRES Calle San Lorenzo, 4292-Munro-Buenos Aires-Argentina
P: 11-4762-6556 F: 11-4762-6466 C: 54

Brazil:

NSK BRASIL LTDA. www.br.nsk.com
SÃO PAULO Rua Treze de Maio, 1633-14° andar-Bela Vista São Paulo-SP, Brazil 01327-905
P: 011-3269-4723 F: 011-3269-4720 C: 55
SUZANO PLANT Av. Vereador João Batista Fitipaldi, 66-Vila Maluf Suzano-SP, Brazil 08685-000
P: 011-4741-4090 F: 011-4748-2355 C: 55
BELO HORIZONTE Rua Ceará, 1431-4° andar-sala 405-Funcionários Belo Horizonte-MG, Brazil 30150-311
P: 031-3274-2477 F: 031-3273-4408 C: 55
JOINVILLE Rua Blumenau, 178-sala 910-Centro Joinville-SC, Brazil 89204-250
P: 047-422-5445/433-3627 F: 047-422-2817 C: 55
PORTO ALEGRE Av. Cristovão Colombo, 1694-sala 202-Floresta Porto Alegre-RS, Brazil 90560 001
P: 051-3222-1324/3346-7851 F: 051-3222-2599 C: 55
RECIFE Av. Conselheiro Aguiar, 2738-6° andar-conj. 604-Boa Viagem Recife-PE, Brazil 51020-020
P: 081-3326-3781 F: 081-3326-5047 C: 55

Canada:

NSK CANADA INC. www.ca.nsk.com
HEAD OFFICE 5585 McAdam Road, Mississauga, Ontario L4Z 1N4, Canada
P: 905-890-0740 F: 905-890-0434 C: 1
MONTREAL 2150-32E Avenue, Lachine, Quebec H8T 3H7, Canada
P: 514-633-1220 F: 514-633-8164 C: 1
TORONTO 5585 McAdam Road, Mississauga, Ontario L4Z 1N4, Canada
P: 905-890-0561 F: 905-890-1938 C: 1
EDMONTON 9267-41st Avenue, Edmonton, Alberta T6E 6R5, Canada
P: 604-294-1151 F: 604-294-1407 C: 1
VANCOUVER 3353 Wayburne Drive, Burnaby, British Columbia V5G 4L4, Canada
P: 604-294-1151 F: 604-294-1407 C: 1

Mexico:

NSK RODAMIENTOS MEXICANA, S.A. DE C.V. www.mx.nsk.com
MEXICO CITY Minas Palacio No.42-6, Col. San Antonio Zomeyucan, Naucalpan de Juarez, C.P. 53750, Estado de Mexico, Mexico
P: 55-301-2741, 55-301-3115, 55-301-4762 F: 55-301-2244, 55-301-2865 C: 52

United States of America:

NSK CORPORATION www.nsk-corp.com
[CORPORATE OFFICE]
ANN ARBOR 4200 Goss Road, Ann Arbor, MI 48105-2703
P: 734-913-7500 F: 734-913-7511 C: 1

[NSK AMERICAN TECHNICAL CENTER]
ANN ARBOR 4200 Goss Road, Ann Arbor, MI 48105-2703
P: 734-913-7500 F: 734-913-7852 C: 1

[BRANCHES and DISTRIBUTION CENTERS]
CERRITOS 13921 Bettencourt Street, Cerritos, California 90703, U.S.A.
P: 562-926-2975 F: 562-926-3553 C: 1
PLAINFIELD 1581 S. Perry Road, Plainfield, Indiana 46168, U.S.A.
P: 317-837-8879 F: 317-837-7207 C: 1

[PLANTS]
ANN ARBOR 5400 South State Road, Ann Arbor, Michigan 48108-9794, U.S.A.
P: 734-996-4400 F: 734-996-4707 C: 1
CLARINDA 1100 North First Street, Clarinda, Iowa 51632-1983, U.S.A.
P: 712-542-5121 F: 712-542-4905 C: 1
FRANKLIN 3400 Bearing Drive, Franklin, Indiana 46131-9660, U.S.A.
P: 317-738-5000 F: 317-738-4310 C: 1
LIBERTY 1112 East Kitchel Road, Liberty, Indiana 47353-8985, U.S.A.
P: 765 458-5000 F: 765 458-7832 C: 1

NSK PRECISION AMERICA, INC. www.npa.nsk.com
CHICAGO 2171 Executive Drive, Suite 100 Addison, Illinois 60101-5600, U.S.A.
P: 630-620-8500 F: 630-620-8555 C: 1
SAN JOSE 780 Montague Expressway, Suite 508, San Jose, Ca 95131
P: 408-944-9400 F: 408-944-9405 C: 1

NSK STEERING SYSTEMS AMERICA, INC. www.nastech.nsk.com
CORPORATE / OFFICE/PLANT / SALES OFFICE 110 Shields Drive Route 2, Box 0030, Bennington, Vermont 05201-8309, U.S.A.
P: 802-442-5448 F: 802-442-2253 C: 1
4200 Goss Road, P.O. Box 134007, Ann Arbor, MI 48113-4007
P: 734-913-7500 F: 734-913-7328 C: 1

NSK LATIN AMERICA, INC. www.latinamerica.nsk.com
MIAMI 2500 NW 107 Avenue, Suite 300, Miami, Florida, 33172, U.S.A.
P: (305) 477-0605 F: (305) 477-0377 C: 1

P: Phone F: Fax T: Telex C: Country Code

Printed in Japan

Motion & Control

No.15 December 2003

Published by NSK Ltd.